

HYBRID FINITE DIFFERENCE SCHEME FOR ELLIPTIC INTERFACE PROBLEMS WITH DISCONTINUOUS AND HIGH-CONTRAST VARIABLE COEFFICIENTS

QIWEI FENG, BIN HAN, AND PETER MINEV

ABSTRACT. For elliptic interface problems with discontinuous coefficients, the maximum accuracy order for compact 9-point finite difference scheme in irregular points is three [7]. The discontinuous coefficients usually have abrupt jumps across the interface curve in the porous medium of realistic problems, causing the pollution effect of numerical methods. So, to obtain a reasonable numerical solution of the above problem, the higher order scheme and its effective implementation are necessary. In this paper, we propose an efficient and flexible way to achieve the implementation of a hybrid (9-point scheme with sixth order accuracy for interior regular points and 13-point scheme with fifth order accuracy for interior irregular points) finite difference scheme in uniform meshes for the elliptic interface problems with discontinuous and high-contrast piecewise smooth coefficients in a rectangle Ω . We also derive the 6-point and 4-point finite difference schemes in uniform meshes with sixth order accuracy for the side points and corner points of various mixed boundary conditions (Dirichlet, Neumann and Robin) of elliptic equations in a rectangle. Our numerical experiments confirm the flexibility and the sixth order accuracy in l_2 and l_∞ norms of the proposed hybrid scheme.

1. INTRODUCTION AND MOTIVATIONS

Elliptic interface problems with discontinuous coefficients appear in many real-world applications: composite materials, fluid mechanics, nuclear waste disposal, and many others. One possible avenue to solve such problems, the so-called immersed interface method (IIM), is proposed by LeVeque and Li. It has been combined with finite difference, finite volume, and finite element spatial discretizations, with various degree of accuracy. Some of the most important developments include: the second order IIM [1, 15], the second order immersed finite volume element methods [3], the second order immersed finite element methods [9, 10], the second order fast iterative immersed interface methods of [13], the second order explicit-jump immersed interface methods of [20], the third order compact finite difference scheme of [17] and fourth order IIM of [25].

Another possible approach for the resolution of elliptic interface problems with discontinuous coefficients is the matched interface and boundary methods (MIB). The related papers of MIB for the elliptic interface problems can be summarized as: second order MIB [21], fourth order MIB [24], fourth order MIB with the FFT acceleration [4], sixth order MIB [22, 23]. For the anisotropic elliptic interface problems with discontinuous and matrix coefficients, [2] proposed a new finite element-finite difference (FE-FD) method with a second order of accuracy.

In [7] we developed a compact 9-point finite difference scheme for elliptic problems, that is formally fourth order accurate away from the interface of singularity of the solution (regular points), and third order accurate in the vicinity of this interface (irregular points). The numerical experiments in [7] demonstrate that the proposed scheme is fourth order accuracy in the l_2 norm. Since the maximum accuracy for compact 9-point finite difference stencil at regular points is six, and a 13-point stencil at irregular points can achieve a fifth order of accuracy, in the present paper we derive a hybrid scheme that utilizes a 9-point stencil for regular points and a 13-point stencil for irregular points, for the

2010 *Mathematics Subject Classification.* 65N06, 35J15, 76S05, 41A58.

Key words and phrases. Elliptic interface problems, hybrid finite difference schemes, fifth or sixth order accuracy, mixed boundary conditions, corner treatments, high-contrast coefficients, discontinuous and variable coefficients.

Research supported in part by Natural Sciences and Engineering Research Council (NSERC) of Canada under grants RGPIN-2019-04276 (Bin Han), RGPIN-2017-04152 (Peter Minev), Westgrid (www.westgrid.ca), and Compute Canada Calcul Canada (www.computecanada.ca).

case of elliptic problems with discontinuous scalar coefficients. In [7] we demonstrated that if the coefficient of the problem is continuous the stencil of a 9-point scheme in 2D can be partitioned into 72 different configurations by the interface of singularity of the solution. In the case of discontinuous coefficients, we need to use a 13-point stencil at irregular points and this results in more possibilities for the stencil partitioning (see figure 1). Thus, in the present paper we also derive an efficient way to achieve the implementation of the proposed hybrid scheme.

A comprehensive literature review of the finite difference approximation of mixed boundary conditions in rectangular domains can be found in [14]. In addition, one should also mention the following literature concerned with the discretization of the boundary conditions for elliptic problems: the sixth order 6-point finite difference scheme for 1-side Neumann and 3-side Dirichlet boundary conditions of Helmholtz equations with constant wave numbers [16], the sixth order 5-point or 6-point finite difference schemes for 1-side Neumann/Robin and 3-side Dirichlet boundary conditions of Helmholtz equations with variable wave numbers [19], the fourth order MIB for 4-side Robin boundary conditions of elliptic interface problems [4], up to 8th order MIB for mixed boundary conditions of Dirichlet, Neumann and Robin with all constant coefficients of Poisson/Helmholtz equations [5].

Compact finite differences have also been successfully applied to elliptic problems with various boundary conditions in non-rectangular domains. In [18] a fourth order MIB for Dirichlet, Neumann, and Robin boundary conditions has been proposed. [20] developed a second order explicit-jump immersed interface method for problems with Dirichlet and Neumann boundary conditions, and [11, 12] proposed fourth order compact finite difference schemes for various combinations of boundary conditions .

In [8], we discussed the 6-point and 4-point finite difference schemes with sixth order accuracy for the side points and corner points of the Helmholtz equations respectively with a constant wave number k in a rectangle. In this paper, we also extend the above results in [8] to the elliptic equations with variable coefficients and mixed combinations of Dirichlet $u|_{\Gamma_i} = g_i$, Neumann $\frac{\partial u}{\partial \bar{n}}|_{\Gamma_j} = g_j$ and Robin $\frac{\partial u}{\partial \bar{n}} + \alpha u|_{\Gamma_k} = g_k$ with smooth functions α , g_i , g_j and g_k , where $\Gamma_i/\Gamma_j/\Gamma_k$ for $i, j, k = 1, 2, 3, 4$ is one side of the rectangle (see Fig. 2 for an example of the mixed boundary conditions).

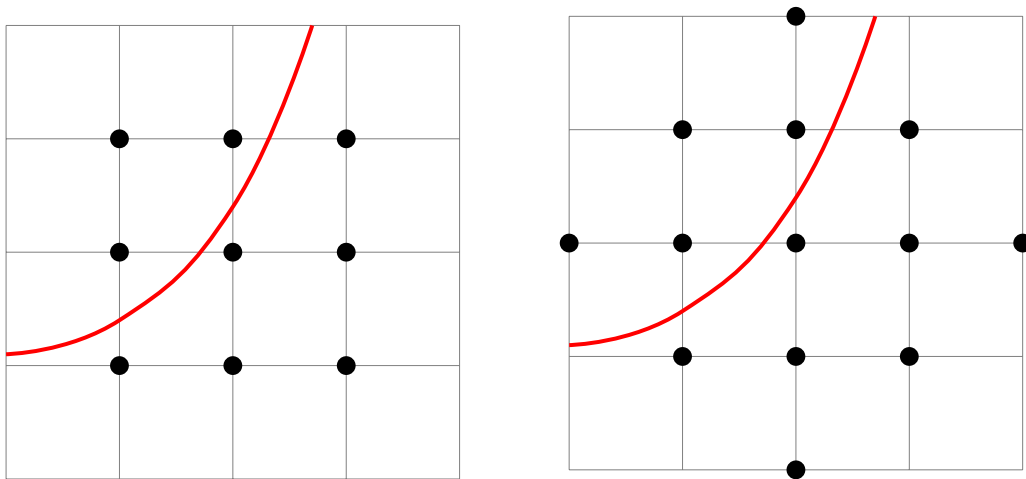


FIGURE 1. For irregular points, the 9-point scheme (left) and the 13-point scheme (right). The curve in red color is the interface curve Γ_I .

In order to define the subject of the present paper, let $\Omega = (l_1, l_2) \times (l_3, l_4)$ and ψ be a smooth two-dimensional function. Consider a smooth curve $\Gamma_I := \{(x, y) \in \Omega : \psi(x, y) = 0\}$, which partitions Ω into two subregions: $\Omega^+ := \{(x, y) \in \Omega : \psi(x, y) > 0\}$ and $\Omega^- := \{(x, y) \in \Omega : \psi(x, y) < 0\}$. We also define $a_{\pm} := a\chi_{\Omega^{\pm}}$, $f_{\pm} := f\chi_{\Omega^{\pm}}$ and $u_{\pm} := u\chi_{\Omega^{\pm}}$. The model problem in this paper is defined as

follows:

$$\begin{cases} -\nabla \cdot (a\nabla u) = f & \text{in } \Omega \setminus \Gamma_I, \\ [u] = g_D, \quad [a\nabla u \cdot \vec{n}] = g_N & \text{on } \Gamma_I, \\ \mathcal{B}_1 u = g_1 \text{ on } \Gamma_1 := \{l_1\} \times (l_3, l_4), \quad \mathcal{B}_2 u = g_2 \text{ on } \Gamma_2 := \{l_2\} \times (l_3, l_4), \\ \mathcal{B}_3 u = g_3 \text{ on } \Gamma_3 := (l_1, l_2) \times \{l_3\}, \quad \mathcal{B}_4 u = g_4 \text{ on } \Gamma_4 := (l_1, l_2) \times \{l_4\}, \end{cases} \quad (1.1)$$

where f is the source term, and for any point $(x_0, y_0) \in \Gamma_I$,

$$\begin{aligned} [u](x_0, y_0) &:= \lim_{(x,y) \in \Omega^+, (x,y) \rightarrow (x_0, y_0)} u(x, y) - \lim_{(x,y) \in \Omega^-, (x,y) \rightarrow (x_0, y_0)} u(x, y), \\ [a\nabla u \cdot \vec{n}](x_0, y_0) &:= \lim_{(x,y) \in \Omega^+, (x,y) \rightarrow (x_0, y_0)} a\nabla u(x, y) \cdot \vec{n} - \lim_{(x,y) \in \Omega^-, (x,y) \rightarrow (x_0, y_0)} a\nabla u(x, y) \cdot \vec{n}, \end{aligned}$$

where \vec{n} is the unit normal vector of Γ_I pointing towards Ω^+ . In (1.1), the boundary operators $\mathcal{B}_1, \dots, \mathcal{B}_4 \in \{\mathbf{I}_d, \frac{\partial}{\partial \vec{n}} + \alpha \mathbf{I}_d\}$, where \mathbf{I}_d represents the Dirichlet boundary condition, when $\alpha = 0$, $\frac{\partial}{\partial \vec{n}}$ represents the Neumann boundary condition, when α is a smooth 1D function, $\frac{\partial}{\partial \vec{n}} + \alpha \mathbf{I}_d$ represents the Robin boundary condition. An example for the boundary conditions of (1.1) is shown in Fig. 2.

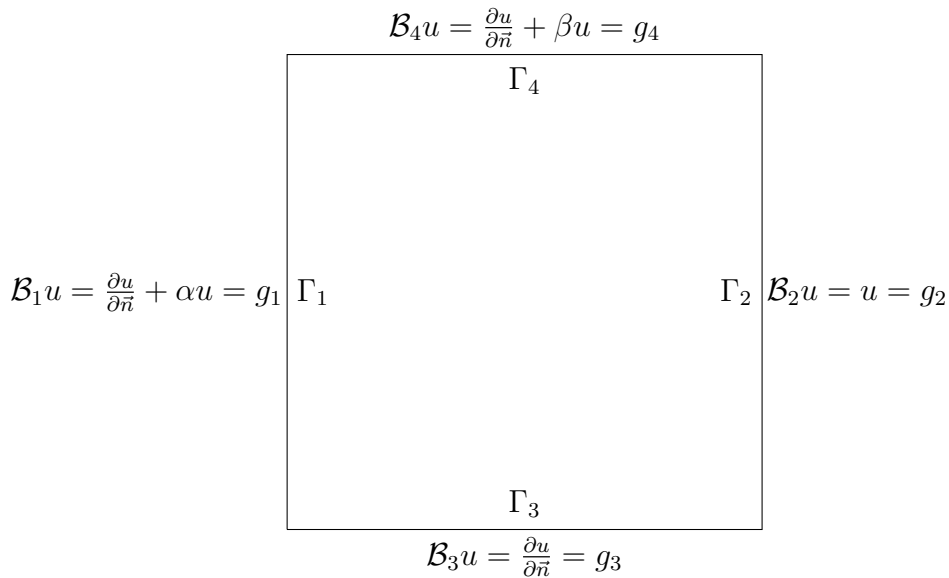


FIGURE 2. An example for the boundary configuration in (1.1), where α and β are two smooth 1D functions in y and x directions respectively.

We derive a hybrid finite difference scheme to solve (1.1) given the following assumptions:

- (A1) The coefficient a is positive, piecewise smooth and has uniformly continuous partial derivatives of (total) orders up to six in each of the subregions Ω^+ and Ω^- . The coefficient a is discontinuous across the interface Γ_I .
- (A2) The solution u and the source term f have uniformly continuous partial derivatives of (total) orders up to seven and five respectively in each of the subregions Ω^+ and Ω^- . Both u and f can be discontinuous across the interface Γ_I .
- (A3) The interface curve Γ_I is smooth in the sense that for each $(x^*, y^*) \in \Gamma_I$, there exists a local parametric equation: $\gamma : (-\epsilon, \epsilon) \rightarrow \Gamma_I$ with $\epsilon > 0$ such that $\gamma(0) = (x^*, y^*)$ and $\|\gamma'(0)\|_2 \neq 0$.
- (A4) The 1D interface functions $g_D \circ \gamma$ and $g_N \circ \gamma$ have uniformly continuous derivatives of (total) orders up to five and four respectively on the interface Γ_I , where γ is given in (A2).
- (A5) Each of the 1D boundary functions g_1, \dots, g_4 in (1.1) and α in the Robin boundary conditions has uniformly continuous derivatives of (total) order up to five on the boundary Γ_j .

The organization of this paper is as follows.

In Section 2.1, we derive the compact 9-point finite difference scheme with sixth order accuracy for regular points in Theorem 2.1.

In Section 2.2.1, we propose the 6-point schemes with sixth order accuracy for the side points of the boundary conditions $\frac{\partial u}{\partial \bar{n}} + \alpha u|_{\Gamma_1} = g_1$, $\frac{\partial u}{\partial \bar{n}}|_{\Gamma_3} = g_3$ and $\frac{\partial u}{\partial \bar{n}} + \beta u|_{\Gamma_4} = g_4$ in Theorems 2.2 to 2.4 with two smooth functions α and β .

In Section 2.2.2, we construct the 4-point schemes with sixth order accuracy for the corner points of the boundary conditions $\frac{\partial u}{\partial \bar{n}} + \alpha u|_{\Gamma_1} = g_1$, $\frac{\partial u}{\partial \bar{n}}|_{\Gamma_3} = g_3$ and $\frac{\partial u}{\partial \bar{n}} + \beta u|_{\Gamma_4} = g_4$ in Theorems 2.5 and 2.6 with two smooth functions α and β .

In Section 2.3, we first propose a simpler version of the transmission equation for the interface curve Γ_I in Theorem 2.7. Then the 13-point finite difference scheme with fifth order accuracy for irregular points is shown in Theorem 2.8. In order to achieve the implementation effectively for the 13-point scheme, we derive efficient implementation details using (2.33) to (2.42).

In Section 3, we present 10 numerical examples, including 5 examples with exact known solutions u , for our proposed hybrid finite difference scheme with contrast ratios $\sup(a_+)/\inf(a_-) = 10^{-3}, 10^{-6}, 10^6, 10^7$. Our numerical experiments confirm the flexibility and the sixth order accuracy in l_2 and l_∞ norms of our proposed hybrid scheme. For the coefficients $a(x, y)$, two jump functions g_D, g_N , interface curves Γ_I and boundary conditions, we test the following cases:

- Either a_+/a_- or a_-/a_+ is very large on the interface Γ_I for high contrast coefficients a .
- The jump functions g_D and g_N are both either constant or non-constant.
- The interface curve Γ_I is either smooth or sharp-edged.
- 4-side Dirichlet boundary conditions.
- 3-side Dirichlet and 1-side Robin boundary conditions.
- 1-side Dirichlet, 1-side Neumann and 2-side Robin boundary conditions.

In Section 4, we summarize the main contributions of this paper. Finally, in Section 5 we present the proofs for results stated in Section 2.

2. HYBRID FINITE DIFFERENCE METHOD ON UNIFORM CARTESIAN GRIDS

We follow the same setup as in [6, 7, 8]. Let $\Omega = (l_1, l_2) \times (l_3, l_4)$ and we assume $l_4 - l_3 = N_0(l_2 - l_1)$ for some $N_0 \in \mathbb{N}$. For any positive integer $N_1 \in \mathbb{N}$, we define $N_2 := N_0 N_1$ and so the grid size is $h := (l_2 - l_1)/N_1 = (l_4 - l_3)/N_2$. Let

$$x_i = l_1 + ih, \quad i = 0, \dots, N_1, \quad \text{and} \quad y_j = l_3 + jh, \quad j = 0, \dots, N_2. \quad (2.1)$$

Recall that a compact stencil centered at (x_i, y_j) contains nine points $(x_i + kh, y_j + lh)$ for $k, l \in \{-1, 0, 1\}$. Define

$$\begin{aligned} d_{i,j}^+ &:= \{(k, \ell) : k, \ell \in \{-1, 0, 1\}, \psi(x_i + kh, y_j + \ell h) \geq 0\}, \quad \text{and} \\ d_{i,j}^- &:= \{(k, \ell) : k, \ell \in \{-1, 0, 1\}, \psi(x_i + kh, y_j + \ell h) < 0\}. \end{aligned} \quad (2.2)$$

Thus, the interface curve $\Gamma_I := \{(x, y) \in \Omega : \psi(x, y) = 0\}$ splits the nine points in our compact stencil into two disjoint sets $\{(x_{i+k}, y_{j+\ell}) : (k, \ell) \in d_{i,j}^+\} \subseteq \Omega^+ \cup \Gamma_I$ and $\{(x_{i+k}, y_{j+\ell}) : (k, \ell) \in d_{i,j}^-\} \subseteq \Omega^-$. We refer to a grid/center point (x_i, y_j) as a *regular point* if $d_{i,j}^+ = \emptyset$ or $d_{i,j}^- = \emptyset$. The center point (x_i, y_j) of a stencil is *regular* if all of its nine points are in $\Omega^+ \cup \Gamma_I$ (hence $d_{i,j}^- = \emptyset$) or in Ω^- (i.e., $d_{i,j}^+ = \emptyset$). Otherwise, if both $d_{i,j}^+$ and $d_{i,j}^-$ are nonempty, the center point (x_i, y_j) of a stencil is referred to as an *irregular point*.

Now, let us pick and fix a base point (x_i^*, y_j^*) inside the open square $(x_i - h, x_i + h) \times (y_j - h, y_j + h)$, which can be written as

$$x_i^* = x_i - v_0 h \quad \text{and} \quad y_j^* = y_j - w_0 h \quad \text{with} \quad -1 < v_0, w_0 < 1. \quad (2.3)$$

Throughout the paper, we shall use the following notations:

$$\begin{aligned} \alpha^{(n)} &:= \frac{d^n \alpha}{dy^n}(y_j^*), & g_1^{(n)} &:= \frac{d^n g_1}{dy^n}(y_j^*), \\ \beta^{(m)} &:= \frac{d^m \beta}{dx^m}(x_i^*), & g_3^{(m)} &:= \frac{d^m g_3}{dx^m}(x_i^*), & g_4^{(m)} &:= \frac{d^m g_4}{dx^m}(x_i^*), \\ a^{(m,n)} &:= \frac{\partial^{m+n} a}{\partial^m x \partial^n y}(x_i^*, y_j^*), & u^{(m,n)} &:= \frac{\partial^{m+n} u}{\partial^m x \partial^n y}(x_i^*, y_j^*), & f^{(m,n)} &:= \frac{\partial^{m+n} f}{\partial^m x \partial^n y}(x_i^*, y_j^*), \end{aligned} \quad (2.4)$$

which are their (m, n) th partial derivatives at the base point (x_i^*, y_j^*) . By [7, (2.13)], we have

$$u(x + x_i^*, y + y_j^*) = \sum_{(m,n) \in \Lambda_{M+1}^{V,1}} u^{(m,n)} G_{M,m,n}^V(x, y) + \sum_{(m,n) \in \Lambda_{M-1}} f^{(m,n)} Q_{M,m,n}^V(x, y) + \mathcal{O}(h^{M+2}), \quad (2.5)$$

for $x, y \in (-2h, 2h)$, where u is the exact solution for (1.1), the index sets Λ_{M-1} and $\Lambda_{M+1}^{V,1}$ are defined in (5.1) and (5.2) respectively, and the functions $G_{M,m,n}^V$ and $Q_{M,m,n}^V$ are defined in (5.4) and (5.5) respectively. By [8, (2.13) and (2.14)], we also have

$$u(x + x_i^*, y + y_j^*) = \sum_{(m,n) \in \Lambda_{M+1}^{H,1}} u^{(m,n)} G_{M,m,n}^H(x, y) + \sum_{(m,n) \in \Lambda_{M-1}} f^{(m,n)} Q_{M,m,n}^H(x, y) + \mathcal{O}(h^{M+2}), \quad (2.6)$$

where the index sets Λ_{M-1} and $\Lambda_{M+1}^{H,1}$ are defined in (5.1) and (5.3) respectively, and the functions $G_{M,m,n}^H$ and $Q_{M,m,n}^H$ are defined in (5.6) and (5.7) respectively.

For the sake of better readability, all technical proofs of this section are provided in Section 5.

2.1. Stencils for regular points (interior). We now extend the fourth order compact scheme in [7, Theorem 3.1] to a sixth order compact scheme. We only need to choose $M = 6$ and replace $G_{m,n}$, $H_{m,n}$ and Λ_{M+1}^1 in [7] by $G_{M,m,n}^V$ in (5.4), $Q_{M,m,n}^V$ in (5.5), and $\Lambda_{M+1}^{V,1}$ in (5.2). We choose (x_i^*, y_j^*) to be the center point of the 9-point compact scheme, i.e., $(x_i^*, y_j^*) = (x_i, y_j)$ and $v_0 = w_0 = 0$ in (2.3).

Theorem 2.1. *Let a grid point (x_i, y_j) be a regular point, i.e., either $d_{i,j}^+ = \emptyset$ or $d_{i,j}^- = \emptyset$ and $(x_i, y_j) \notin \partial\Omega$. Let $(u_h)_{i,j}$ denote the numerical approximation of the exact solution u of the elliptic interface problem (1.1) at an interior regular point (x_i, y_j) . Then the following difference scheme on a stencil centered at (x_i, y_j) :*

$$\begin{aligned} & C_{-1,-1}(u_h)_{i-1,j-1} + C_{0,-1}(u_h)_{i,j-1} + C_{1,-1}(u_h)_{i+1,j-1} \\ \mathcal{L}_h u_h := & + C_{-1,0}(u_h)_{i-1,j} + C_{0,0}(u_h)_{i,j} + C_{1,0}(u_h)_{i+1,j} = \sum_{(m,n) \in \Lambda_5} f^{(m,n)} C_{f,m,n}, \\ & + C_{-1,1}(u_h)_{i-1,j+1} + C_{0,1}(u_h)_{i,j+1} + C_{1,1}(u_h)_{i+1,j+1} \end{aligned} \quad (2.7)$$

achieves sixth order of accuracy for $-\nabla \cdot (a \nabla u) = f$ at the point (x_i, y_j) , where

$$\begin{aligned} C_{f,m,n} &:= \sum_{k=-1}^1 \sum_{\ell=-1}^1 C_{k,\ell} Q_{6,m,n}^V(kh, \ell h), \quad \text{for all } (m,n) \in \Lambda_5, \\ C_{k,\ell}(h) &:= \sum_{i=0}^{M+1} c_{k,\ell,i} h^i, \quad k, \ell \in \{-1, 0, 1\}, \end{aligned} \quad (2.8)$$

and $\{c_{k,\ell,i}\}$ is any non-trivial solution to the linear system induced by [7, (3.5)] with $M = 6$. Moreover, the maximum accuracy order of a compact finite difference scheme for $-\nabla \cdot (a \nabla u) = f$ at the point (x_i, y_j) is six.

To verify Theorem 2.1 with the numerical experiments in Section 3, we use the unique solution $\{c_{k,\ell,i}\}$ to [7, (3.5)] with $M = 6$ and the normalization condition $c_{-1,-1,0} = 1$, setting to zero all $c_{-1,0,7}$, $c_{0,-1,7}$, $c_{0,0,6}$, $c_{0,0,7}$, $c_{-1,1,i_1}$, $c_{0,1,i_2}$, $c_{1,-1,i_2}$, $c_{1,0,i_3}$, $c_{1,1,i_4}$ for $i_1 = 1, 6, 7$, $i_2 = 5, 6, 7$, $i_3 = 4, 5, 6, 7$ and $i_4 = 2, 3, 4, 5, 6, 7$.

2.2. Stencils for boundary points. In this subsection, we extend [8, Section 2.2] and discuss how to find a compact finite difference scheme with accuracy order six centered at $(x_i, y_j) \in \partial\Omega$. For clarity of presentation, we consider the following boundary conditions

$$\begin{aligned} \mathcal{B}_1 u &= \frac{\partial u}{\partial \bar{n}} + \alpha u = g_1 \quad \text{on } \Gamma_1, & \mathcal{B}_2 u &= u = g_2 \quad \text{on } \Gamma_2, \\ \mathcal{B}_3 u &= \frac{\partial u}{\partial \bar{n}} = g_3 \quad \text{on } \Gamma_3, & \mathcal{B}_4 u &= \frac{\partial u}{\partial \bar{n}} + \beta u = g_4 \quad \text{on } \Gamma_4, \end{aligned} \quad (2.9)$$

where α and β are two smooth 1D functions in y and x directions. For the 6-point and 4-point schemes in this subsection, we choose $(x_i^*, y_j^*) = (x_i, y_j)$ and $v_0 = w_0 = 0$ in (2.3). An illustration of (2.9) is shown in Fig. 2. For the following identities in (2.12) and (2.18), we define

$$\delta_{a,a} := 1 \quad \text{and} \quad \delta_{a,b} := 0 \quad \text{for } a \neq b. \quad (2.10)$$

2.2.1. Side points on the boundary $\partial\Omega$.

Theorem 2.2. *Let $(u_h)_{i,j}$ denote the numerical approximation of the exact solution u of the elliptic interface problem (1.1) at the point (x_i, y_j) . The following discretization on a stencil centered at $(x_0, y_j) \in \Gamma_1$:*

$$\begin{aligned} \mathcal{L}_h^{\mathcal{B}_1} u_h &:= +C_{0,-1}^{\mathcal{B}_1}(u_h)_{0,j-1} + C_{1,-1}^{\mathcal{B}_1}(u_h)_{1,j-1} \\ &+ C_{0,0}^{\mathcal{B}_1}(u_h)_{0,j} + C_{1,0}^{\mathcal{B}_1}(u_h)_{1,j} \\ &+ C_{0,1}^{\mathcal{B}_1}(u_h)_{0,j+1} + C_{1,1}^{\mathcal{B}_1}(u_h)_{1,j+1} \end{aligned} = \sum_{(m,n) \in \Lambda_4} f^{(m,n)} C_{f,m,n}^{\mathcal{B}_1} + \sum_{n=0}^5 g_1^{(n)} C_{g_1,n}^{\mathcal{B}_1}, \quad (2.11)$$

achieves sixth order of accuracy for $\mathcal{B}_1 u = \frac{\partial u}{\partial \bar{n}} + \alpha u = g_1$ at the point $(x_0, y_j) \in \Gamma_1$, where

$$C_{f,m,n}^{\mathcal{B}_1} := \sum_{k=0}^1 \sum_{\ell=-1}^1 C_{k,\ell}^{\mathcal{B}_1} Q_{5,m,n}^V(kh, \ell h), \quad \text{for all } (m,n) \in \Lambda_4,$$

$$C_{g_1,n}^{\mathcal{B}_1} := - \sum_{k=0}^1 \sum_{\ell=-1}^1 C_{k,\ell}^{\mathcal{B}_1} G_{5,1,n}^V(kh, \ell h), \quad \text{for all } n = 0, \dots, 5,$$

$$C_{k,\ell}^{\mathcal{B}_1}(h) := \sum_{i=0}^6 c_{k,\ell,i}^{\mathcal{B}_1} h^i, \quad k \in \{0, 1\}, \ell \in \{-1, 0, 1\},$$

and $\{c_{k,\ell,i}^{\mathcal{B}_1}\}$ is any non-trivial solution to the linear system induced by

$$\begin{aligned} &\sum_{k=0}^1 \sum_{\ell=-1}^1 C_{k,\ell}^{\mathcal{B}_1} \left(G_{5,0,n}^V(kh, \ell h) + \sum_{i=n}^5 \binom{i}{n} \alpha^{(i-n)} G_{5,1,i}^V(kh, \ell h) (1 - \delta_{n,6}) \right) \\ &= \mathcal{O}(h^7), \quad \text{for all } n = 0, 1, \dots, 6. \end{aligned} \quad (2.12)$$

Moreover, the maximum accuracy order of a 6-point finite difference scheme for $\mathcal{B}_1 u = \frac{\partial u}{\partial \bar{n}} + \alpha u = g_1$ at the point $(x_0, y_j) \in \Gamma_1$ with two smooth functions $\alpha(y)$ and $a(x, y)$ is six.

In our numerical experiments in Section 3, we use the unique solution $\{c_{k,\ell,i}^{\mathcal{B}_1}\}$ to (2.12) with the normalization condition $c_{1,1,0}^{\mathcal{B}_1} = 1$, where all $c_{0,0,6}^{\mathcal{B}_1}, c_{0,1,5}^{\mathcal{B}_1}, c_{0,1,6}^{\mathcal{B}_1}, c_{1,-1,i_1}^{\mathcal{B}_1}, c_{1,0,i_2}^{\mathcal{B}_1}, c_{1,1,i_3}^{\mathcal{B}_1}$ for $i_1 = 1, 4, 5, 6$, $i_2 = 3, 4, 5, 6$, and $i_3 = 2, 3, 4, 5, 6$, are set to zero. In particular, if a in (1.1) is a discontinuous constant coefficient and $\mathcal{B}_1 u = \frac{\partial u}{\partial \bar{n}} + \alpha u = g_1$ with a constant α , then the coefficients in (2.11) are

$$\begin{aligned} C_{0,1}^{\mathcal{B}_1} &= \frac{1}{75} \alpha^2 h^2 + \frac{1}{5} \alpha h + 2, \quad C_{0,0}^{\mathcal{B}_1} = \frac{8}{675} \alpha^5 h^5 - \frac{16}{675} \alpha^4 h^4 + \frac{16}{225} \alpha^3 h^3 - \frac{8}{25} \alpha^2 h^2 - \frac{34}{5} \alpha h - 10, \\ C_{1,1}^{\mathcal{B}_1} &= 1, \quad C_{1,0}^{\mathcal{B}_1} = -\frac{8}{675} \alpha^4 h^4 + \frac{8}{225} \alpha^3 h^3 - \frac{8}{75} \alpha^2 h^2 + \frac{2}{5} \alpha h + 4, \quad C_{0,-1}^{\mathcal{B}_1} = C_{0,1}^{\mathcal{B}_1}, \quad C_{1,-1}^{\mathcal{B}_1} = C_{1,1}^{\mathcal{B}_1}. \end{aligned} \quad (2.13)$$

Similarly, we could obtain the following Theorems 2.3 and 2.4.

Theorem 2.3. Let $(u_h)_{i,j}$ be the numerical approximation of the exact solution u of the elliptic interface problem (1.1) at the point (x_i, y_j) . Then the following discretization stencil centered at $(x_i, y_0) \in \Gamma_3$:

$$\mathcal{L}_h^{\mathcal{B}_3} u_h := \begin{array}{c} C_{-1,0}^{\mathcal{B}_3}(u_h)_{i-1,0} + C_{0,0}^{\mathcal{B}_3}(u_h)_{i,0} + C_{1,0}^{\mathcal{B}_3}(u_h)_{i+1,0} \\ + C_{-1,1}^{\mathcal{B}_3}(u_h)_{i-1,1} + C_{0,1}^{\mathcal{B}_3}(u_h)_{i,1} + C_{1,1}^{\mathcal{B}_3}(u_h)_{i+1,1} \end{array} = \sum_{(m,n) \in \Lambda_4} f^{(m,n)} C_{f,m,n}^{\mathcal{B}_3} + \sum_{n=0}^5 g_3^{(n)} C_{g_3,n}^{\mathcal{B}_3}, \quad (2.14)$$

achieves sixth order of accuracy for $\mathcal{B}_3 u = \frac{\partial u}{\partial \bar{n}} = g_3$ at the point $(x_i, y_0) \in \Gamma_3$, where

$$C_{f,m,n}^{\mathcal{B}_3} := \sum_{k=-1}^1 \sum_{\ell=0}^1 C_{k,\ell}^{\mathcal{B}_3} Q_{5,m,n}^H(kh, \ell h), \quad \text{for all } (m,n) \in \Lambda_4,$$

$$C_{g_3,n}^{\mathcal{B}_3} := - \sum_{k=-1}^1 \sum_{\ell=0}^1 C_{k,\ell}^{\mathcal{B}_3} G_{5,n,1}^H(kh, \ell h), \quad \text{for all } n = 0, \dots, 5,$$

$$C_{k,\ell}^{\mathcal{B}_3}(h) := \sum_{i=0}^6 c_{k,\ell,i}^{\mathcal{B}_3} h^i, \quad k \in \{-1, 0, 1\}, \ell \in \{0, 1\},$$

and $\{c_{k,\ell,i}^{\mathcal{B}_3}\}$ is any non-trivial solution to the linear system induced by

$$\sum_{k=-1}^1 \sum_{\ell=0}^1 C_{k,\ell}^{\mathcal{B}_3} G_{5,n,0}^H(kh, \ell h) = \mathcal{O}(h^7), \quad \text{for all } n = 0, 1, \dots, 6, \quad (2.15)$$

Moreover, the maximum accuracy order of a 6-point finite difference scheme for $\mathcal{B}_3 u = \frac{\partial u}{\partial \bar{n}} = g_3$ at the point $(x_i, y_0) \in \Gamma_3$ with a smooth function $a(x, y)$ is six.

For our numerical experiments in Section 3, we use the unique solution $\{c_{k,\ell,i}^{\mathcal{B}_3}\}$ to (2.15) with the normalization condition $c_{1,1,0}^{\mathcal{B}_3} = 1$, presetting to zero all $c_{0,0,6}^{\mathcal{B}_3}, c_{-1,1,i_1}^{\mathcal{B}_3}, c_{0,1,i_2}^{\mathcal{B}_3}, c_{1,0,i_3}^{\mathcal{B}_3}, c_{1,1,i_4}^{\mathcal{B}_3}$ for $i_1 = 1, 5, 6$, $i_2 = 4, 5, 6$, $i_3 = 3, 4, 5, 6$, and $i_4 = 2, 3, 4, 5, 6$. In particular, if a is a discontinuous constant coefficient in (1.1), then the coefficients in (2.14) are

$$C_{1,0}^{\mathcal{B}_3} = 2, \quad C_{1,1}^{\mathcal{B}_3} = 1, \quad C_{0,0}^{\mathcal{B}_3} = -10, \quad C_{0,1}^{\mathcal{B}_3} = 4, \quad C_{-1,0}^{\mathcal{B}_3} = C_{1,0}^{\mathcal{B}_3}, \quad C_{-1,1}^{\mathcal{B}_3} = C_{1,1}^{\mathcal{B}_3}. \quad (2.16)$$

Theorem 2.4. Let $(u_h)_{i,j}$ be the numerical approximation of the exact solution u of the elliptic interface problem (1.1) at the point (x_i, y_j) . Then the following discretization stencil centered at $(x_i, y_{N_2}) \in \Gamma_4$:

$$\mathcal{L}_h^{\mathcal{B}_4} u_h := \begin{array}{c} C_{-1,-1}^{\mathcal{B}_4}(u_h)_{i-1,-1} + C_{0,-1}^{\mathcal{B}_4}(u_h)_{i,-1} + C_{1,-1}^{\mathcal{B}_4}(u_h)_{i+1,-1} \\ + C_{-1,0}^{\mathcal{B}_4}(u_h)_{i-1,0} + C_{0,0}^{\mathcal{B}_4}(u_h)_{i,0} + C_{1,0}^{\mathcal{B}_4}(u_h)_{i+1,0} \end{array} = \sum_{(m,n) \in \Lambda_4} f^{(m,n)} C_{f,m,n}^{\mathcal{B}_4} + \sum_{n=0}^5 g_4^{(n)} C_{g_4,n}^{\mathcal{B}_4}, \quad (2.17)$$

achieves sixth order of accuracy for $\mathcal{B}_4 u = \frac{\partial u}{\partial \bar{n}} + \beta u = g_4$ at the point $(x_i, y_{N_2}) \in \Gamma_4$, where

$$C_{f,m,n}^{\mathcal{B}_4} := \sum_{k=-1}^1 \sum_{\ell=-1}^0 C_{k,\ell}^{\mathcal{B}_4} Q_{5,m,n}^H(kh, \ell h), \quad \text{for all } (m,n) \in \Lambda_4,$$

$$C_{g_4,n}^{\mathcal{B}_4} := \sum_{k=-1}^1 \sum_{\ell=-1}^0 C_{k,\ell}^{\mathcal{B}_4} G_{5,n,1}^H(kh, \ell h), \quad \text{for all } n = 0, \dots, 5,$$

$$C_{k,\ell}^{\mathcal{B}_4}(h) := \sum_{i=0}^6 c_{k,\ell,i}^{\mathcal{B}_4} h^i, \quad k \in \{-1, 0, 1\}, \ell \in \{-1, 0\},$$

and $\{c_{k,\ell,i}^{\mathcal{B}_4}\}$ is any non-trivial solution to the linear system induced by

$$\begin{aligned} & \sum_{k=-1}^1 \sum_{\ell=-1}^0 C_{k,\ell}^{\mathcal{B}_4} \left(G_{5,n,0}^H(kh, \ell h) - \sum_{i=n}^5 \binom{i}{n} \beta^{(i-n)} G_{5,i,1}^H(kh, \ell h) (1 - \delta_{n,6}) \right) \\ & = \mathcal{O}(h^7), \quad \text{for all } n = 0, 1, \dots, 6. \end{aligned} \quad (2.18)$$

Moreover, the maximum accuracy order of a 6-point finite difference scheme for $\mathcal{B}_4 u = \frac{\partial u}{\partial \bar{n}} + \beta u = g_4$ at the point $(x_i, y_{N_2}) \in \Gamma_4$ with two smooth functions $\beta(x)$ and $a(x, y)$ is six.

For our numerical experiments in Section 3, we use the unique solution $\{c_{k,\ell,i}^{\mathcal{B}_4}\}$ to (2.18) with the normalization condition $c_{1,-1,0}^{\mathcal{B}_4} = 1$, presetting to zero all $c_{0,-1,6}^{\mathcal{B}_4}, c_{-1,0,5}^{\mathcal{B}_4}, c_{-1,0,6}^{\mathcal{B}_4}, c_{0,0,i_1}^{\mathcal{B}_4}, c_{1,-1,i_2}^{\mathcal{B}_4}, c_{1,0,i_3}^{\mathcal{B}_4}$ with $i_1 = 4, 5, 6, i_2 = 2, 3, 4, 5, 6, i_3 = 1, 3, 4, 5, 6$. In particular, if a is a discontinuous piecewise constant coefficient and $\mathcal{B}_4 u = \frac{\partial u}{\partial \bar{n}} + \beta u = g_4$ with a constant β , then the coefficients in (2.17) are

$$\begin{aligned} C_{1,-1}^{\mathcal{B}_4} &= 1, \quad C_{0,-1}^{\mathcal{B}_4} = -\frac{8}{675}\beta^4 h^4 + \frac{8}{225}\beta^3 h^3 - \frac{8}{75}\beta^2 h^2 + \frac{2}{5}\beta h + 4, \\ C_{1,0}^{\mathcal{B}_4} &= \frac{1}{75}\beta^2 h^2 + \frac{1}{5}\beta h + 2, \quad C_{0,0}^{\mathcal{B}_4} = \frac{8}{675}\beta^5 h^5 - \frac{16}{675}\beta^4 h^4 + \frac{16}{225}\beta^3 h^3 - \frac{8}{25}\beta^2 h^2 - \frac{34}{5}\beta h - 10, \\ C_{-1,-1}^{\mathcal{B}_4} &= C_{1,-1}^{\mathcal{B}_4}, \quad C_{-1,0}^{\mathcal{B}_4} = C_{1,0}^{\mathcal{B}_4}. \end{aligned} \quad (2.19)$$

2.2.2. Stencils for corner points.

Theorem 2.5. *Let $(u_h)_{i,j}$ be the numerical approximation of the exact solution u of the elliptic interface problem (1.1) at the point (x_i, y_j) . Then the following discretization on a stencil centered at the corner point (x_0, y_0) :*

$$\mathcal{L}_h^{\mathcal{R}_1} u_h := \begin{array}{l} C_{0,0}^{\mathcal{R}_1}(u_h)_{0,0} + C_{1,0}^{\mathcal{R}_1}(u_h)_{1,0} \\ + C_{0,1}^{\mathcal{R}_1}(u_h)_{0,1} + C_{1,1}^{\mathcal{R}_1}(u_h)_{1,1} \end{array} = \sum_{(m,n) \in \Lambda_4} f^{(m,n)} C_{f,m,n}^{\mathcal{R}_1} + \sum_{n=0}^5 g_1^{(n)} C_{g_1,n}^{\mathcal{R}_1} + \sum_{n=0}^5 g_3^{(n)} C_{g_3,n}^{\mathcal{R}_1}, \quad (2.20)$$

achieves sixth order of accuracy for $\mathcal{B}_1 u = \frac{\partial u}{\partial \bar{n}} + \alpha u = g_1$ and $\mathcal{B}_3 u = \frac{\partial u}{\partial \bar{n}} = g_3$ at the point (x_0, y_0) , where $\{C_{k,\ell}^{\mathcal{R}_1}\}_{k,\ell \in \{0,1\}}$, $\{C_{f,m,n}^{\mathcal{R}_1}\}_{(m,n) \in \Lambda_4}$, $\{C_{g_1,n}^{\mathcal{R}_1}\}_{n=0}^5$ and $\{C_{g_3,n}^{\mathcal{R}_1}\}_{n=0}^5$ can be calculated by replacing $\mathcal{B}_1 u = \frac{\partial u}{\partial \bar{n}} - iku = g_1$ by $\mathcal{B}_1 u = \frac{\partial u}{\partial \bar{n}} + \alpha u = g_1$ in [8, Theorem 2.4] with $M = M_f = M_{g_1} = M_{g_3} = 5$, and replacing $G_{M,m,n}^V, Q_{M,m,n}^V, G_{M,m,n}^H$ and $Q_{M,m,n}^H$ in [8] by (5.4), (5.5), (5.6) and (5.7), respectively. Moreover, the maximum accuracy order of a 4-point finite difference scheme for $\mathcal{B}_1 u = \frac{\partial u}{\partial \bar{n}} + \alpha u = g_1$ and $\mathcal{B}_3 u = \frac{\partial u}{\partial \bar{n}} = g_3$ at the point (x_0, y_0) with two smooth functions $\alpha(y)$ and $a(x, y)$ is six.

In particular, if a in (1.1) is a discontinuous piecewise constant coefficient, and $\mathcal{B}_1 u = \frac{\partial u}{\partial \bar{n}} + \alpha u = g_1$ with a constant α , then the coefficients in (2.20) are

$$\begin{aligned} C_{0,0}^{\mathcal{R}_1} &= \frac{4}{675}\alpha^5 h^5 - \frac{8}{675}\alpha^4 h^4 + \frac{8}{225}\alpha^3 h^3 - \frac{4}{25}\alpha^2 h^2 - \frac{17}{5}\alpha h - 5, \quad C_{0,1}^{\mathcal{R}_1} = \frac{1}{75}\alpha^2 h^2 + \frac{1}{5}\alpha h + 2, \\ C_{1,0}^{\mathcal{R}_1} &= -\frac{4}{675}\alpha^4 h^4 + \frac{4}{225}\alpha^3 h^3 - \frac{4}{75}\alpha^2 h^2 + \frac{1}{5}\alpha h + 2, \quad C_{1,1}^{\mathcal{R}_1} = 1. \end{aligned} \quad (2.21)$$

Theorem 2.6. *Let $(u_h)_{i,j}$ be the numerical approximation of the exact solution u of the elliptic interface problem (1.1) at the point (x_i, y_j) . Then the following discretization on a stencil centered at the corner point (x_0, y_{N_2}) :*

$$\mathcal{L}_h^{\mathcal{R}_2} u_h := \begin{array}{l} C_{0,-1}^{\mathcal{R}_2}(u_h)_{0,N_2-1} + C_{1,-1}^{\mathcal{R}_2}(u_h)_{1,N_2-1} \\ + C_{0,0}^{\mathcal{R}_2}(u_h)_{0,N_2} + C_{1,0}^{\mathcal{R}_2}(u_h)_{1,N_2} \end{array} = \sum_{(m,n) \in \Lambda_4} f^{(m,n)} C_{f,m,n}^{\mathcal{R}_2} + \sum_{n=0}^5 g_1^{(n)} C_{g_1,n}^{\mathcal{R}_2} + \sum_{n=0}^5 g_4^{(n)} C_{g_4,n}^{\mathcal{R}_2}, \quad (2.22)$$

achieves sixth order of accuracy for $\mathcal{B}_1 u = \frac{\partial u}{\partial \bar{n}} + \alpha u = g_1$ and $\mathcal{B}_4 u = \frac{\partial u}{\partial \bar{n}} + \beta u = g_4$ at the point (x_0, y_{N_2}) , where $\{C_{k,\ell}^{\mathcal{R}_2}\}_{k \in \{0,1\}, \ell \in \{-1,0\}}$, $\{C_{f,m,n}^{\mathcal{R}_2}\}_{(m,n) \in \Lambda_4}$, $\{C_{g_1,n}^{\mathcal{R}_2}\}_{n=0}^5$ and $\{C_{g_4,n}^{\mathcal{R}_2}\}_{n=0}^5$ can be calculated by replacing $\mathcal{B}_1 u = \frac{\partial u}{\partial \bar{n}} - iku = g_1$ and $\mathcal{B}_4 u = \frac{\partial u}{\partial \bar{n}} - iku = g_4$ by $\mathcal{B}_1 u = \frac{\partial u}{\partial \bar{n}} + \alpha u = g_1$ and $\mathcal{B}_4 u = \frac{\partial u}{\partial \bar{n}} + \beta u = g_4$ respectively in [8, Theorem 2.5] with $M = M_f = M_{g_1} = M_{g_4} = 5$ and replacing $G_{M,m,n}^V, Q_{M,m,n}^V,$

$G_{M,m,n}^H$ and $Q_{M,m,n}^H$ in [8] by (5.4), (5.5), (5.6) and (5.7), respectively. Moreover, the maximum accuracy order of a 4-point finite difference scheme for $\mathcal{B}_1 u = \frac{\partial u}{\partial \bar{n}} + \alpha u = g_1$ and $\mathcal{B}_4 u = \frac{\partial u}{\partial \bar{n}} + \beta u = g_4$ at the point (x_0, y_{N_2}) with three smooth functions $\alpha(y)$, $\beta(x)$ and $a(x, y)$ is six, where $\alpha(y_{N_2}) \neq \beta(x_0)$.

Again, if a in (1.1) is a discontinuous constant coefficient, $\mathcal{B}_1 u = \frac{\partial u}{\partial \bar{n}} + \alpha u = g_1$ and $\mathcal{B}_4 u = \frac{\partial u}{\partial \bar{n}} + \beta u = g_4$ with α and β being constant, then the coefficients on the left hand side in (2.22) are

$$\begin{aligned}
C_{0,-1}^{\mathcal{R}_2} &= \frac{1}{675}(4\alpha^5 - 6\alpha^4\beta + 6\alpha^3\beta^2 - 4\alpha^2\beta^3)h^5 + \frac{1}{675}(4\alpha^4 - 6\alpha^3\beta + 6\alpha^2\beta^2 - 4\alpha\beta^3)h^4 \\
&\quad + \frac{1}{675}(9\alpha^2 + 63\alpha\beta - 36\beta^2)h^2 + \frac{1}{675}(135\beta + 135\alpha)h + 2, \\
C_{0,0}^{\mathcal{R}_2} &= \frac{1}{225}(-4\alpha^4 + 6\alpha^3\beta - 6\alpha^2\beta^2 + 4\alpha\beta^3)h^4 + \frac{1}{225}(8\alpha^3 - 18\alpha^2\beta - 30\alpha\beta^2 + 16\beta^3)h^3 \\
&\quad + \frac{1}{225}(-36\alpha^2 - 357\alpha\beta - 36\beta^2)h^2 + \frac{1}{225}(-765\alpha - 765\beta)h - 5, \\
C_{1,-1}^{\mathcal{R}_2} &= \frac{1}{675}(-4\alpha^4 + 6\alpha^3\beta - 6\alpha^2\beta^2 + 4\alpha\beta^3)h^4 + 1, \\
C_{1,0}^{\mathcal{R}_2} &= \frac{1}{225}(4\alpha^3 - 6\alpha^2\beta + 6\alpha\beta^2 - 4\beta^3)h^3 + \frac{1}{225}(-12\alpha^2 + 21\alpha\beta + 3\beta^2)h^2 \\
&\quad + \frac{1}{225}(45\beta + 45\alpha)h + 2.
\end{aligned} \tag{2.23}$$

When $\alpha = \beta$, we further have $C_{0,-1}^{\mathcal{R}_2} = C_{1,0}^{\mathcal{R}_2} = \frac{4}{75}\beta^2 h^2 + \frac{2}{5}\beta h + 2$ and $C_{1,-1}^{\mathcal{R}_2} = 1$ in (2.23).

2.3. Stencils for irregular points. Let (x_i, y_j) be an irregular point (i.e., both $d_{i,j}^+$ and $d_{i,j}^-$ are nonempty, see Fig. 1 for an example) and choose the base point $(x_i^*, y_j^*) \in \Gamma_I \cap (x_i - h, x_i + h) \times (y_j - h, y_j + h)$. By (2.3), we have

$$x_i^* = x_i - v_0 h \quad \text{and} \quad y_j^* = y_j - w_0 h \quad \text{with} \quad -1 < v_0, w_0 < 1 \quad \text{and} \quad (x_i^*, y_j^*) \in \Gamma_I. \tag{2.24}$$

Let a_{\pm} , u_{\pm} and f_{\pm} represent the coefficient function a , the solution u and source term f in Ω^{\pm} . Similar to (2.4), we define that

$$\begin{aligned}
a_{\pm}^{(m,n)} &:= \frac{\partial^{m+n} a_{\pm}}{\partial^m x \partial^n y}(x_i^*, y_j^*), & u_{\pm}^{(m,n)} &:= \frac{\partial^{m+n} u_{\pm}}{\partial^m x \partial^n y}(x_i^*, y_j^*), & f_{\pm}^{(m,n)} &:= \frac{\partial^{m+n} f_{\pm}}{\partial^m x \partial^n y}(x_i^*, y_j^*), \\
g_D^{(m,n)} &:= \frac{\partial^{m+n} g_D}{\partial^m x \partial^n y}(x_i^*, y_j^*), & g_N^{(m,n)} &:= \frac{\partial^{m+n} g_N}{\partial^m x \partial^n y}(x_i^*, y_j^*).
\end{aligned}$$

Similar to (2.5), we have

$$u_{\pm}(x + x_i^*, y + y_j^*) = \sum_{(m,n) \in \Lambda_{M+1}^{V,1}} u_{\pm}^{(m,n)} G_{M,m,n}^{\pm,V}(x, y) + \sum_{(m,n) \in \Lambda_{M-1}} f_{\pm}^{(m,n)} Q_{M,m,n}^{\pm,V}(x, y) + \mathcal{O}(h^{M+2}),$$

for $x, y \in (-2h, 2h)$, where Λ_{M-1} and $\Lambda_{M+1}^{V,1}$ are defined in (5.1) and (5.2) respectively, $G_{M,m,n}^{\pm,V}(x, y)$ and $Q_{M,m,n}^{\pm,V}(x, y)$ are obtained by replacing $\{a^{(m,n)} : (m, n) \in \Lambda_M\}$ by $\{a_{\pm}^{(m,n)} : (m, n) \in \Lambda_M\}$ in (5.4) and (5.5). As in [6, 7, 8], near the point (x_i^*, y_j^*) , the parametric equation of Γ_I can be written as:

$$x = r(t) + x_i^*, \quad y = s(t) + y_j^*, \quad (r'(t))^2 + (s'(t))^2 > 0 \quad \text{for } t \in (-\epsilon, \epsilon) \quad \text{with } \epsilon > 0, \tag{2.25}$$

where r and s are smooth functions. Similarly to the definition of the 9-point compact stencil in (2.2), we define the following 4-point set for the 13-point scheme:

$$\begin{aligned}
e_{i,j}^+ &:= \{(k, \ell) : (k, \ell) \in \{(-2, 0), (0, -2), (0, 2), (2, 0)\}, \psi(x_i + kh, y_j + \ell h) \geq 0\}, \quad \text{and} \\
e_{i,j}^- &:= \{(k, \ell) : (k, \ell) \in \{(-2, 0), (0, -2), (0, 2), (2, 0)\}, \psi(x_i + kh, y_j + \ell h) < 0\}.
\end{aligned} \tag{2.26}$$

In the next theorem we present a simplified version of [7, Theorem 3.2], adapted to the aim of developing of a fifth order hybrid 13-point scheme for irregular points.

Theorem 2.7. *Let u be the solution to the elliptic interface problem in (1.1) and let Γ_I be parameterized near (x_i^*, y_j^*) by (2.25). Then*

$$\begin{aligned} u_-^{(m',n')} &= \sum_{\substack{(m,n) \in \Lambda_{M+1}^{V,1} \\ m+n \leq m'+n'}} T_{m',n',m,n}^{u+} u_+^{(m,n)} + \sum_{(m,n) \in \Lambda_{M-1}} \left(T_{m',n',m,n}^+ f_+^{(m,n)} + T_{m',n',m,n}^- f_-^{(m,n)} \right) \\ &+ \sum_{(m,n) \in \Lambda_{M+1}} T_{m',n',m,n}^{g_D} g_D^{(m,n)} + \sum_{(m,n) \in \Lambda_M} T_{m',n',m,n}^{g_N} g_N^{(m,n)}, \quad \forall (m',n') \in \Lambda_{M+1}^{V,1}, \end{aligned} \quad (2.27)$$

where all the transmission coefficients $T^{u+}, T^{\pm}, T^{g_D}, T^{g_N}$ are uniquely determined by $r^{(k)}(0), s^{(k)}(0)$ for $k = 0, \dots, M+1$ and $\{a_{\pm}^{(m,n)} : (m,n) \in \Lambda_M\}$. Moreover, let $T_{m',n',m,n}^{u+}$ be the transmission coefficient of $u_+^{(m,n)}$ in (2.27) with $(m,n) \in \Lambda_{M+1}^{V,1}$, $m+n = m'+n'$ and $(m',n') \in \Lambda_{M+1}^{V,1}$. Then $T_{m',n',m,n}^{u+}$ only depends on $r^{(k)}(0), s^{(k)}(0)$ for $k = 0, \dots, M+1$ of (2.25) and $a_{\pm}^{(0,0)}$. Particularly,

$$T_{0,0,0,0}^{u+} = 1 \quad \text{and} \quad T_{m',n',0,0}^{u+} = 0 \quad \text{if } (m',n') \neq (0,0). \quad (2.28)$$

Next, we provide the 13-point finite difference scheme for interior irregular points.

Theorem 2.8. *Let $(u_h)_{i,j}$ be the numerical approximation to the solution of (1.1) at an interior irregular point (x_i, y_j) . Pick a base point (x_i^*, y_j^*) as in (2.24). Then the following 13-point scheme centered at the interior irregular point (x_i, y_j) :*

$$\begin{aligned} \mathcal{L}_h^{\Gamma_I} := & \begin{array}{ccccccc} & & & C_{0,-2}(u_h)_{i,j-2} & & & \\ & & & +C_{-1,-1}(u_h)_{i-1,j-1} & +C_{0,-1}(u_h)_{i,j-1} & +C_{1,-1}(u_h)_{i+1,j-1} & \\ +C_{-2,0}(u_h)_{i-2,j} & +C_{-1,0}(u_h)_{i-1,j} & +C_{0,0}(u_h)_{i,j} & +C_{1,0}(u_h)_{i+1,j} & +C_{2,0}(u_h)_{i+2,j} & & \\ & +C_{-1,1}(u_h)_{i-1,j+1} & +C_{0,1}(u_h)_{i,j+1} & +C_{1,1}(u_h)_{i+1,j+1} & & & \\ & & & +C_{0,2}(u_h)_{i,j+2} & & & \end{array} \\ & \quad (2.29) \end{aligned}$$

$$= \sum_{(m,n) \in \Lambda_3} f_+^{(m,n)} J_{m,n}^+ + \sum_{(m,n) \in \Lambda_3} f_-^{(m,n)} J_{m,n}^- + \sum_{(m,n) \in \Lambda_5} g_D^{(m,n)} J_{m,n}^{g_D} + \sum_{(m,n) \in \Lambda_4} g_N^{(m,n)} J_{m,n}^{g_N},$$

achieves fifth order accuracy, where all $\{C_{k,\ell}\}$ in (2.29) are calculated by (2.41), $J_{m,n}^{\pm} := J_{m,n}^{\pm,0} + J_{m,n}^{\pm,T}$ for all $(m,n) \in \Lambda_3$,

$$\begin{aligned} J_{m,n}^{\pm,0} &:= \sum_{(k,\ell) \in d_{i,j}^{\pm} \cup e_{i,j}^{\pm}} C_{k,\ell} Q_{4,m,n}^{\pm,V}((v_0+k)h, (w_0+\ell)h), \quad J_{m,n}^{\pm,T} := \sum_{(m',n') \in \Lambda_5^{V,1}} I_{m',n'}^- T_{m',n',m,n}^{\pm}, \quad \forall (m,n) \in \Lambda_3, \\ J_{m,n}^{g_D} &:= \sum_{(m',n') \in \Lambda_5^{V,1}} I_{m',n'}^- T_{m',n',m,n}^{g_D}, \quad \forall (m,n) \in \Lambda_5, \quad J_{m,n}^{g_N} := \sum_{(m',n') \in \Lambda_5^{V,1}} I_{m',n'}^- T_{m',n',m,n}^{g_N}, \quad \forall (m,n) \in \Lambda_4, \\ I_{m,n}^- &:= \sum_{(k,\ell) \in d_{i,j}^- \cup e_{i,j}^-} C_{k,\ell} G_{4,m,n}^-, \quad \forall (m,n) \in \Lambda_5^{V,1}. \end{aligned}$$

Moreover, the maximum accuracy order of a 13-point finite difference stencil for (1.1) at an interior irregular point (x_i, y_j) is five.

For the 13-point scheme in Theorem 2.8, if only one point in the set $\{(x_i-h, y_j-h), (x_i-h, y_j+h), (x_i+h, y_j-h), (x_i+h, y_j+h)\}$ belongs to Ω^- and the other 12 points all belong to Ω^+ , we can set $C_{k,\ell} = 0$ for $(x_i+kh, y_j+\ell h) \in \Omega^-$, $x_i^* = x_i, y_i^* = y_i$ to achieve sixth order accuracy in (x_i, y_j) .

Finally, we provide a way of achieving an efficient implementation for the 13-point scheme in irregular points in Theorem 2.8.

Efficient implementation details:

By Theorem 2.7, a simpler $J_{m,n}^{u+,T}(h)$ in [7, (3.26)] can be written as:

$$J_{m,n}^{u+,T}(h) := \sum_{\substack{(m',n') \in \Lambda_{M+1}^{V,1} \\ m'+n' \geq m+n}} I_{m',n'}^-(h) T_{m',n',m,n}^{u+}. \quad (2.30)$$

Replacing Λ_{M+1}^1 by $\Lambda_{M+1}^{V,1}$ for [7, (3.28) and (3.29)], we have

$$I_{m,n}^+(h) + J_{m,n}^{u+,T}(h) = \mathcal{O}(h^{M+2}), \quad h \rightarrow 0, \quad \text{for all } (m,n) \in \Lambda_{M+1}^{V,1}. \quad (2.31)$$

Replacing $G_{m,n}^\pm$, $H_{m,n}^\pm$ and $d_{i,j}^\pm$ by $G_{M,m,n}^{\pm,V}$, $Q_{M,m,n}^{\pm,V}$ and $d_{i,j}^\pm \cup e_{i,j}^\pm$ for [7, (3.25) and (3.26)], we obtain

$$\sum_{(k,\ell) \in d_{i,j}^+ \cup e_{i,j}^+} C_{k,\ell}(h) G_{M,m,n}^{+,V}(v_0h + kh, w_0h + \ell h) + \sum_{\substack{(m',n') \in \Lambda_{M+1}^{V,1} \\ m'+n' \geq m+n}} I_{m',n'}^-(h) T_{m',n',m,n}^{u+} = \mathcal{O}(h^{M+2}),$$

and

$$\begin{aligned} & \sum_{(k,\ell) \in d_{i,j}^+ \cup e_{i,j}^+} C_{k,\ell}(h) G_{M,m,n}^{+,V}(v_0h + kh, w_0h + \ell h) \\ & + \sum_{\substack{(m',n') \in \Lambda_{M+1}^{V,1} \\ m'+n' \geq m+n}} \sum_{(k,\ell) \in d_{i,j}^- \cup e_{i,j}^-} C_{k,\ell}(h) G_{M,m',n'}^{-,V}(v_0h + kh, w_0h + \ell h) T_{m',n',m,n}^{u+} = \mathcal{O}(h^{M+2}). \end{aligned}$$

So, (2.31) is equivalent to

$$\begin{aligned} & \sum_{(k,\ell) \in d_{i,j}^- \cup e_{i,j}^-} C_{k,\ell}(h) \sum_{\substack{(m',n') \in \Lambda_{M+1}^{V,1} \\ m'+n' \geq m+n}} G_{M,m',n'}^{-,V}(v_0h + kh, w_0h + \ell h) T_{m',n',m,n}^{u+} \\ & + \sum_{(k,\ell) \in d_{i,j}^+ \cup e_{i,j}^+} C_{k,\ell}(h) G_{M,m,n}^{+,V}(v_0h + kh, w_0h + \ell h) = \mathcal{O}(h^{M+2}), \quad \text{for all } (m,n) \in \Lambda_{M+1}^{V,1}. \end{aligned} \quad (2.32)$$

Let

$$C_{k,\ell}(h) := \sum_{i=0}^{M+1} c_{k,\ell,i} h^i, \quad X_{k,\ell} := (c_{k,\ell,0}, c_{k,\ell,1}, \dots, c_{k,\ell,M+1})^T. \quad (2.33)$$

Since $G_{M,m,n}^{\pm,V}((k+v_0)h, (\ell+w_0)h)$ is the polynomial of h and the degree of h of every term in $G_{M,m,n}^{\pm,V}((k+v_0)h, (\ell+w_0)h)$ is non-negative, we deduce that

$$C_{k,\ell}(h) G_{M,m,n}^{+,V}((k+v_0)h, (\ell+w_0)h) = DA_{k,\ell}^{+,m,n} X_{k,\ell} + \mathcal{O}(h^{M+2}), \quad (2.34)$$

$$C_{k,\ell}(h) \sum_{\substack{(m',n') \in \Lambda_{M+1}^{V,1} \\ m'+n' \geq m+n}} G_{M,m',n'}^{-,V}((k+v_0)h, (\ell+w_0)h) T_{m',n',m,n}^{u+} = DA_{k,\ell}^{-,m,n} X_{k,\ell} + \mathcal{O}(h^{M+2}), \quad (2.35)$$

where

$$D = (h^0, h^1, \dots, h^{M+1}),$$

and $A_{k,\ell}^{\pm,m,n}$ is independent for h for all $(m,n) \in \Lambda_{M+1}^{V,1}$. So (2.32) is equivalent to

$$\sum_{(k,\ell) \in d_{i,j}^+ \cup e_{i,j}^+} DA_{k,\ell}^{+,m,n} X_{k,\ell} + \sum_{(k,\ell) \in d_{i,j}^- \cup e_{i,j}^-} DA_{k,\ell}^{-,m,n} X_{k,\ell} = \mathcal{O}(h^{M+2}), \quad \text{for all } (m,n) \in \Lambda_{M+1}^{V,1}. \quad (2.36)$$

Define

$$A_{k,\ell}^{m,n} := \begin{cases} A_{k,\ell}^{+,m,n}, & \text{if } (k,\ell) \in d_{i,j}^+ \cup e_{i,j}^+, \\ A_{k,\ell}^{-,m,n}, & \text{if } (k,\ell) \in d_{i,j}^- \cup e_{i,j}^-. \end{cases} \quad (2.37)$$

Then (2.36) is equivalent to

$$A^{m,n} X = 0, \quad \text{for all } (m,n) \in \Lambda_{M+1}^{V,1},$$

where

$$A^{m,n} = (A_{-1,-1}^{m,n}, A_{-1,0}^{m,n}, A_{-1,1}^{m,n}, A_{0,-1}^{m,n}, A_{0,0}^{m,n}, A_{0,1}^{m,n}, A_{1,-1}^{m,n}, A_{1,0}^{m,n}, A_{1,1}^{m,n}, A_{-2,0}^{m,n}, A_{2,0}^{m,n}, A_{0,-2}^{m,n}, A_{0,2}^{m,n}), \quad (2.38)$$

and

$$X = (X_{-1,-1}^T, X_{-1,0}^T, X_{-1,1}^T, X_{0,-1}^T, X_{0,0}^T, X_{0,1}^T, X_{1,-1}^T, X_{1,0}^T, X_{1,1}^T, X_{-2,0}^T, X_{2,0}^T, X_{0,-2}^T, X_{0,2}^T)^T. \quad (2.39)$$

Let

$$A = ((A^{0,0})^T, (A^{0,1})^T, \dots, (A^{0,M+1})^T, (A^{1,0})^T, (A^{1,1})^T, \dots, (A^{1,M})^T)^T. \quad (2.40)$$

Finally, (2.32) is equivalent to

$$AX = 0. \quad (2.41)$$

Since we use 13-point scheme for the irregular points, we have 13 components in (2.38) and (2.39). If we use 9-point compact scheme for the irregular points, we only need to delete the last four components in (2.38) and (2.39). For the 25-point or 36-point schemes for the irregular points, the only change is to add more $A_{k,\ell}^{m,n}$ and $X_{k,\ell}$ in (2.38) and (2.39). Even there are many different cases for the 13-point schemes for the irregular points depending on how the interface curve Γ_I partitions the 13 points in it, we can repeatedly use $A_{k,\ell}^{\pm,m,n}$ in (2.34), (2.35) and (2.37) to cover all the cases which significantly reduce the computation cost and make the implementation very effective and flexible. Furthermore, if we want to obtain the lower or higher finite schemes for irregular points, we only need to delete or add some $A^{0,n+1}$ and $A^{1,n}$ in (2.40).

After the above simplification, we find that the A in (2.41) is a 36 by 78 matrix for the 13-point scheme with fifth order accuracy while A is a 16 by 36 matrix and the 9-point scheme with third order accuracy. Observing the following identity (whose proof is given in Section 5)

$$c_{0,-2,i} + c_{-2,0,i} + c_{2,0,i} + c_{0,2,i} + \sum_{k=-1}^1 \sum_{\ell=-1}^1 c_{k,\ell,i} = 0, \quad \text{for } i = 0, 1, \dots, M+1, \quad (2.42)$$

we can further reduce the size of the matrix A in (2.41) to 30 by 72 for the 13-point scheme.

3. NUMERICAL EXPERIMENTS

Let $\Omega = (l_1, l_2) \times (l_3, l_4)$ with $l_4 - l_3 = N_0(l_2 - l_1)$ for some positive integer N_0 . For a given $J \in \mathbb{N}_0$, we define $h := (l_2 - l_1)/N_1$ with $N_1 := 2^J$ and let $x_i = l_1 + ih$ and $y_j = l_3 + jh$ for $i = 0, 1, \dots, N_1$ and $j = 0, 1, \dots, N_2$ with $N_2 := N_0 N_1$. Let $u(x, y)$ be the exact solution of (1.1) and $(u_h)_{i,j}$ be a numerical solution at (x_i, y_j) using the mesh size h . We measure the consistency of the proposed scheme in the l_2 norm by the relative error $\frac{\|u_h - u\|_2}{\|u\|_2}$, if the exact solution u is available. If it is not, then we quantify the consistency error by $\|u_h - u_{h/2}\|_2$, where

$$\begin{aligned} \|u_h - u\|_2^2 &:= h^2 \sum_{i=0}^{N_1} \sum_{j=0}^{N_2} ((u_h)_{i,j} - u(x_i, y_j))^2, & \|u\|_2^2 &:= h^2 \sum_{i=0}^{N_1} \sum_{j=0}^{N_2} (u(x_i, y_j))^2, \\ \|u_h - u_{h/2}\|_2^2 &:= h^2 \sum_{i=0}^{N_1} \sum_{j=0}^{N_2} ((u_h)_{i,j} - (u_{h/2})_{2i,2j})^2. \end{aligned}$$

In addition we also provide results for the infinity norm of the errors given by:

$$\|u_h - u\|_\infty := \max_{0 \leq i \leq N_1, 0 \leq j \leq N_2} |(u_h)_{i,j} - u(x_i, y_j)|, \quad \|u_h - u_{h/2}\|_\infty := \max_{0 \leq i \leq N_1, 0 \leq j \leq N_2} |(u_h)_{i,j} - (u_{h/2})_{2i,2j}|.$$

3.1. Numerical examples with known u . In this subsection, we provide five numerical examples with a known solution u of (1.1). Note that the maximum accuracy order for the compact 9-point finite difference scheme in irregular and regular points, for elliptic interface problems with discontinuous coefficients, is three and six, respectively. So, in Examples 3.1 and 3.2 we compare the proposed hybrid scheme with the compact 9-point scheme of a sixth order of accuracy at regular points and third order of accuracy at irregular points. That is, both uses the same compact 9-point stencils with accuracy order six at all regular points, and they only differ at irregular points such that the proposed hybrid scheme uses 13-point stencils having fifth order accuracy, while the compact 9-point scheme uses 9-point stencils having third order accuracy. Their computational costs are comparable, because the percentage of the number of irregular points over all the grid points decays exponentially to 0 at the rate $\mathcal{O}(2^{-J})$, e.g., this percentage is less than or around 1% at the level $J = 9$ for all our numerical examples.

The five numerical examples can be characterized as follows:

- Examples 3.1 and 3.2 compare the proposed hybrid scheme and the 9-point compact scheme.
- In all examples, either a_+/a_- or a_-/a_+ is very large on Γ_I for high contrast coefficients a .
- 4-side Dirichlet boundary conditions are demonstrated in Examples 3.1, 3.2 and 3.5.
- 1-side Dirichlet, 1-side Neumann and 2-side Robin boundary conditions are considered in Examples 3.3 and 3.4.
- Results for smooth interface curves Γ_I are presented in Examples 3.1 and 3.3 to 3.5.
- Results for a sharp-edged interface curve Γ_I are demonstrated in Example 3.2.
- Results for two constant jump functions g_D and g_N are shown in Examples 3.1 and 3.3 to 3.5.
- Results for two non-constant jump functions g_D and g_N are presented in Example 3.2.

Example 3.1. Let $\Omega = (-1.5, 1.5)^2$ and the interface curve be given by $\Gamma_I := \{(x, y) \in \Omega : \psi(x, y) = 0\}$ with $\psi(x, y) = y^2 + \frac{2x^2}{x^2+1} - 1$. The functions in (1.1) are given by

$$\begin{aligned} a_+ &= 10^3(2 + \sin(x)\sin(y)), & a_- &= 10^{-3}(2 + \sin(x)\sin(y)), & g_D &= -200, & g_N &= 0, \\ u_+ &= 10^{-3} \sin(4x) \sin(4y)(y^2(x^2 + 1) + x^2 - 1), \\ u_- &= 10^3 \sin(4x) \sin(4y)(y^2(x^2 + 1) + x^2 - 1) + 200, \\ u(-1.5, y) &= g_1, & u(1.5, y) &= g_2, & \text{for } y &\in (-1.5, 1.5), \\ u(x, -1.5) &= g_3, & u(x, 1.5) &= g_4, & \text{for } x &\in (-1.5, 1.5), \end{aligned}$$

the other functions f^\pm, g_1, \dots, g_4 in (1.1) can be obtained by plugging the above functions into (1.1). Note the high contrast $a_+/a_- = 10^6$ on Γ_I . The numerical results are presented in Table 1 and Fig. 3.

TABLE 1. Performance in Example 3.1 of our proposed hybrid finite difference scheme and compact 9-point scheme on uniform Cartesian meshes with $h = 2^{-J} \times 3$. κ is the condition number of the coefficient matrix.

J	Our proposed hybrid scheme					Compact 9-point scheme				
	$\frac{\ u_h - u\ _2}{\ u\ _2}$	order	$\ u_h - u\ _\infty$	order	κ	$\frac{\ u_h - u\ _2}{\ u\ _2}$	order	$\ u_h - u\ _\infty$	order	κ
4	1.493E-01	0	1.362E+02	0	2.136E+02	5.465E-01	0	4.515E+02	0	8.685E+01
5	3.124E-03	5.6	3.872E+00	5.1	4.262E+02	4.751E-02	3.5	4.453E+01	3.3	4.896E+02
6	6.081E-05	5.7	7.168E-02	5.8	6.261E+03	2.464E-03	4.3	2.890E+00	3.9	2.069E+03
7	1.238E-06	5.6	1.490E-03	5.6	1.701E+04	2.745E-04	3.2	3.318E-01	3.1	9.171E+03
8	1.803E-08	6.1	3.305E-05	5.5	1.169E+05	1.557E-05	4.1	1.894E-02	4.1	4.054E+04
9						9.053E-07	4.1	1.185E-03	4.0	1.648E+05

Example 3.2. Let $\Omega = (-4.5, 4.5)^2$ and the interface curve be given by $\Gamma_I := \{(x, y) \in \Omega : \psi(x, y) = 0\}$ which is shown in Fig. 4. Precisely, the sharp-edged interface is a square with 4 corner points

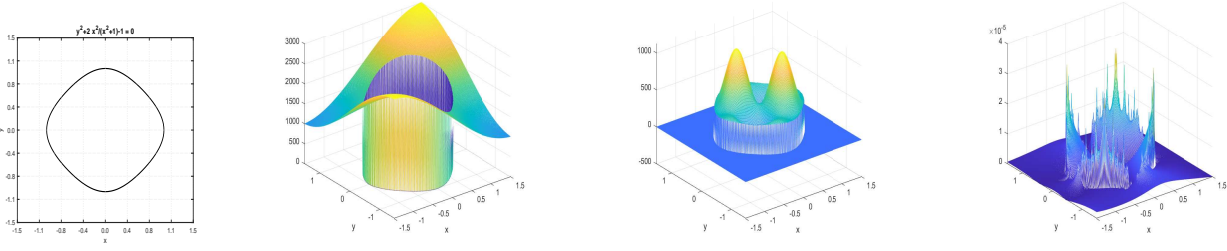


FIGURE 3. Example 3.1: the interface curve Γ_I (first panel), the coefficient $a(x, y)$ (second panel), the numerical solution u_h (third panel), and the error $|u_h - u|$ (fourth panel) with $h = 2^{-8} \times 3$, where u_h is computed by our proposed hybrid finite difference scheme.

$(-2, 0)$, $(0, 2)$, $(2, 0)$ and $(0, -2)$. The functions in (1.1) are given by

$$\begin{aligned} a_+ &= 10^{-3}, & a_- &= 10^3, & u_+ &= 10^3 \sin(x - y), & u_- &= 10^{-3} \cos(x) \cos(y) + 1000, \\ u(-4.5, y) &= g_1, & u(4.5, y) &= g_2, & \text{for } y &\in (-4.5, 4.5), \\ u(x, -4.5) &= g_3, & u(x, 4.5) &= g_4, & \text{for } x &\in (-4.5, 4.5), \end{aligned}$$

the other functions f^\pm , g_D , g_N , g_1, \dots, g_4 in (1.1) can be obtained by plugging the above functions into (1.1). Clearly, g_D and g_N are not constants. Note the high contrast $a_-/a_+ = 10^6$ on Γ_I . The numerical results are presented in Table 2 and Fig. 4.

TABLE 2. Performance in Example 3.2 of our proposed hybrid finite difference scheme and compact 9-point scheme on uniform Cartesian meshes with $h = 2^{-J} \times 9$. κ is the condition number of the coefficient matrix.

J	Our proposed hybrid scheme					Compact 9-point scheme				
	$\frac{\ u_h - u\ _2}{\ u\ _2}$	order	$\ u_h - u\ _\infty$	order	κ	$\frac{\ u_h - u\ _2}{\ u\ _2}$	order	$\ u_h - u\ _\infty$	order	κ
4	7.431E-03	0	2.062E+01	0	1.337E+03	6.254E-02	0	1.574E+02	0	1.238E+03
5	4.505E-04	4.0	1.322E+00	4.0	1.020E+04	1.110E-02	2.5	2.837E+01	2.5	6.529E+03
6	5.701E-06	6.3	1.778E-02	6.2	6.394E+04	6.953E-04	4.0	1.929E+00	3.9	4.152E+04
7	4.937E-08	6.9	1.869E-04	6.6	3.920E+05	2.993E-05	4.5	1.059E-01	4.2	3.286E+05
8	6.087E-10	6.3	2.942E-06	6.0	2.132E+07	1.155E-06	4.7	4.177E-03	4.7	1.474E+06
9						8.390E-08	3.8	3.391E-04	3.6	1.006E+07

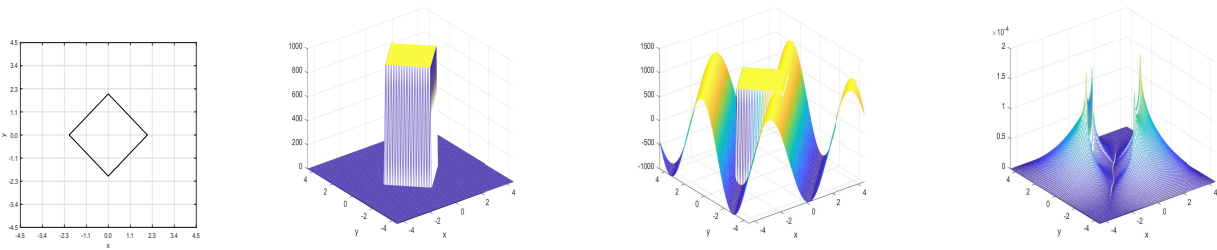


FIGURE 4. Example 3.2: the interface curve Γ_I (first panel), the coefficient $a(x, y)$ (second panel), the numerical solution u_h (third panel), and the error $|u_h - u|$ (fourth panel) with $h = 2^{-7} \times 9$, where u_h is computed by our proposed hybrid finite difference scheme.

Example 3.3. Let $\Omega = (-2.5, 2.5)^2$ and the interface curve be given by $\Gamma_I := \{(x, y) \in \Omega : \psi(x, y) = 0\}$ with $\psi(x, y) = x^4 + 2y^4 - 2$. The functions in (1.1) are given by

$$\begin{aligned} a_+ &= 10^{-3}(2 + \sin(x) \sin(y)), & a_- &= 10^3(2 + \sin(x) \sin(y)), & g_D &= -10^5, & g_N &= 0, \\ u_+ &= 10^3 \sin(4\pi x) \sin(4\pi y)(x^4 + 2y^4 - 2), & u_- &= 10^{-3} \sin(4\pi x) \sin(4\pi y)(x^4 + 2y^4 - 2) + 10^5, \end{aligned}$$

$$\begin{aligned}
& -u_x(-2.5, y) + \alpha u(-2.5, y) = g_1, & u(2.5, y) = g_2, & \alpha = \sin(y), & \text{for } y \in (-2.5, 2.5), \\
& -u_y(x, -2.5) = g_3, & u_y(x, 2.5) + \beta u(x, 2.5) = g_4, & \beta = \cos(x), & \text{for } x \in (-2.5, 2.5),
\end{aligned}$$

the other functions f^\pm, g_1, \dots, g_4 in (1.1) can be obtained by plugging the above functions into (1.1). Note the high contrast $a_-/a_+ = 10^6$ on Γ_I . The numerical results are presented in Table 3 and Fig. 5.

TABLE 3. Performance in Example 3.3 of our proposed hybrid finite difference scheme on uniform Cartesian meshes with $h = 2^{-J} \times 5$.

J	$\frac{\ u_h - u\ _2}{\ u\ _2}$	order	$\ u_h - u\ _\infty$	order	$\ u_h - u_{h/2}\ _2$	order	$\ u_h - u_{h/2}\ _\infty$	order
5	8.167E-01	0	1.758E+05	0	1.811E+05	0	1.734E+05	0
6	1.123E-02	6.2	2.488E+03	6.1	2.471E+03	6.2	2.441E+03	6.2
7	2.059E-04	5.8	4.711E+01	5.7	4.550E+01	5.8	4.640E+01	5.7
8	3.035E-06	6.1	7.028E-01	6.1	6.701E-01	6.1	6.919E-01	6.1
9	4.632E-08	6.0	1.087E-02	6.0	9.946E-03	6.1	1.037E-02	6.1

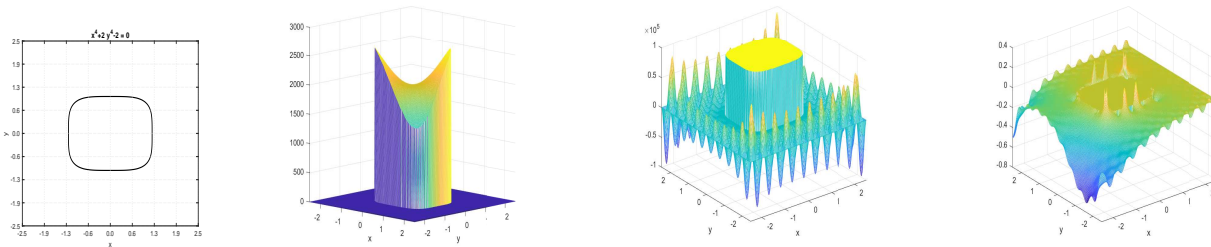


FIGURE 5. Example 3.3: the interface curve Γ_I (first panel), the coefficient $a(x, y)$ (second panel), the numerical solution u_h (third panel), and the error $u - u_h$ (fourth panel) with $h = 2^{-8} \times 5$, where u_h is computed by our proposed hybrid finite difference scheme.

Example 3.4. Let $\Omega = (-2, 2)^2$ and the interface curve be given by $\Gamma_I := \{(x, y) \in \Omega : \psi(x, y) = 0\}$ with $\psi(x, y) = x^2 + y^2 - 2$. The functions in (1.1) are given by

$$\begin{aligned}
& a_+ = 10^3(2 + \sin(x + y)), & a_- = 10^{-3}(2 + \sin(x + y)), & g_D = -10^3, & g_N = 0, \\
& u_+ = 10^{-3} \cos(4(x - y))(x^2 + y^2 - 2), & u_- = 10^3 \cos(4(x - y))(x^2 + y^2 - 2) + 10^3, \\
& -u_x(-2, y) + \alpha u(-2, y) = g_1, & u(2, y) = g_2, & \alpha = \sin(y), & \text{for } y \in (-2, 2), \\
& -u_y(x, -2) = g_3, & u_y(x, 2) + \beta u(x, 2) = g_4, & \beta = \cos(x), & \text{for } x \in (-2, 2),
\end{aligned}$$

the other functions f^\pm, g_1, \dots, g_4 in (1.1) can be obtained by plugging the above functions into (1.1). Note the high contrast $a_+/a_- = 10^6$ on Γ_I . The numerical results are presented in Table 4 and Fig. 6.

TABLE 4. Performance in Example 3.4 of our proposed hybrid finite difference scheme on uniform Cartesian meshes with $h = 2^{-J} \times 4$.

J	$\frac{\ u_h - u\ _2}{\ u\ _2}$	order	$\ u_h - u\ _\infty$	order	$\ u_h - u_{h/2}\ _2$	order	$\ u_h - u_{h/2}\ _\infty$	order
4	8.087E-01	0	4.191E+03	0	2.568E+03	0	4.141E+03	0
5	1.443E-02	5.8	1.061E+02	5.3	4.623E+01	5.8	1.048E+02	5.3
6	2.679E-04	5.8	2.154E+00	5.6	8.629E-01	5.7	2.132E+00	5.6
7	3.432E-06	6.3	3.518E-02	5.9	1.100E-02	6.3	3.477E-02	5.9
8	6.625E-08	5.7	6.192E-04	5.8	2.120E-04	5.7	6.118E-04	5.8

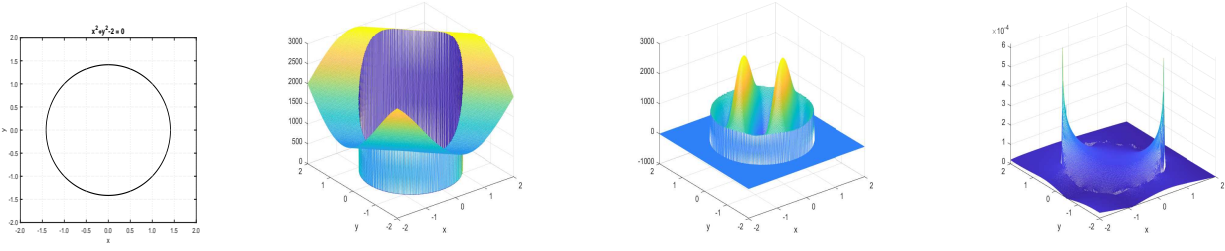


FIGURE 6. Example 3.4: the interface curve Γ_I (first panel), the coefficient $a(x, y)$ (second panel), the numerical solution u_h (third panel), and the error $|u_h - u|$ (fourth panel) with $h = 2^{-8} \times 4$, where u_h is computed by our proposed hybrid finite difference scheme.

Example 3.5. Let $\Omega = (-2.5, 2.5)^2$ and the interface curve be given by $\Gamma_I := \{(x, y) \in \Omega : \psi(x, y) = 0\}$ with $\psi(x, y) = y^2 - 2x^2 + x^4 - \frac{1}{4}$. The functions in (1.1) are given by

$$\begin{aligned} a_+ &= 10^{-3}(2 + \sin(x - y)), & a_- &= 10^3(2 + \sin(x - y)), & g_D &= -1.5 \times 10^4, & g_N &= 0, \\ u_+ &= 10^3 \sin(16(x + y))(y^2 - 2x^2 + x^4 - 1/4), \\ u_- &= 10^{-3} \sin(16(x + y))(y^2 - 2x^2 + x^4 - 1/4) + 1.5 \times 10^4, \\ u(-2.5, y) &= g_1, & u(2.5, y) &= g_2, & \text{for } y &\in (-2.5, 2.5), \\ u(x, -2.5) &= g_3, & u(x, 2.5) &= g_4, & \text{for } x &\in (-2.5, 2.5), \end{aligned}$$

the other functions f^\pm, g_1, \dots, g_4 in (1.1) can be obtained by plugging the above functions into (1.1). Note the high contrast $a_-/a_+ = 10^6$ on Γ_I . The numerical results are presented in Table 5 and Fig. 7.

TABLE 5. Performance in Example 3.5 of our proposed hybrid finite difference scheme on uniform Cartesian meshes with $h = 2^{-J} \times 5$.

J	$\frac{\ u_h - u\ _2}{\ u\ _2}$	order	$\ u_h - u\ _\infty$	order	$\ u_h - u_{h/2}\ _2$	order	$\ u_h - u_{h/2}\ _\infty$	order
5	8.627E-01	0	9.480E+04	0	4.284E+04	0	9.338E+04	0
6	2.854E-02	4.9	2.758E+03	5.1	1.360E+03	5.0	2.736E+03	5.1
7	4.543E-04	6.0	5.673E+01	5.6	2.128E+01	6.0	5.658E+01	5.6
8	6.195E-06	6.2	1.184E+00	5.6	2.856E-01	6.2	1.177E+00	5.6
9	8.902E-08	6.1	1.738E-02	6.1	4.441E-03	6.0	1.788E-02	6.0

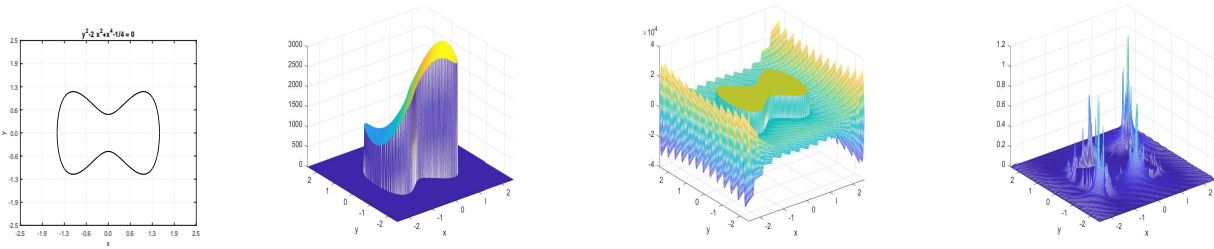


FIGURE 7. Example 3.5: the interface curve Γ_I (first panel), the coefficient $a(x, y)$ (second panel), the numerical solution u_h (third panel), and the error $|u_h - u|$ (fourth panel) with $h = 2^{-8} \times 5$, where u_h is computed by our proposed hybrid finite difference scheme.

3.2. Numerical examples with unknown u . In this subsection, we provide five numerical examples with unknown u of (1.1). They can be characterized as follows.

- In all examples, either a_+/a_- or a_-/a_+ is very large on Γ_I for high-contrast coefficients a .
- 4-side Dirichlet boundary conditions are demonstrated in Examples 3.6 and 3.9.
- 3-side Dirichlet and 1-side Robin boundary conditions in Examples 3.7 and 3.8.

- 1-side Dirichlet, 1-side Neumann and 2-side Robin boundary conditions in Example 3.10.
- All the interface curves Γ_I are smooth and all the jump functions g_D and g_N are non-constant.

Example 3.6. Let $\Omega = (-2.5, 2.5)^2$ and the interface curve be given by $\Gamma_I := \{(x, y) \in \Omega : \psi(x, y) = 0\}$ with $\psi(x, y) = x^4 + 2y^4 - 2$. The functions in (1.1) are given by

$$\begin{aligned} a_+ &= 2 + \cos(x) \cos(y), & a_- &= 10^3(2 + \sin(x) \sin(y)), & g_D &= \sin(x) \sin(y) - 1, \\ f_+ &= \sin(4\pi x) \sin(4\pi y), & f_- &= \cos(4\pi x) \cos(4\pi y), & g_N &= \cos(x) \cos(y), \\ u(-2.5, y) &= 0, & u(2.5, y) &= 0, & \text{for } y &\in (-2.5, 2.5), \\ u(x, -2.5) &= 0, & u(x, 2.5) &= 0, & \text{for } x &\in (-2.5, 2.5). \end{aligned}$$

Note the high contrast $a_-/a_+ \approx 10^3$ on Γ_I . The numerical results are presented in Table 6 and Fig. 8.

TABLE 6. Performance in Example 3.6 of our proposed hybrid finite difference scheme on uniform Cartesian meshes with $h = 2^{-J} \times 5$.

J	$\ u_h - u_{h/2}\ _2$	order	$\ u_h - u_{h/2}\ _\infty$	order
4	9.83385E+02	0	3.29078E+02	0
5	1.93678E+01	5.7	6.50631E+00	5.7
6	3.13024E-01	6.0	1.04785E-01	6.0
8	9.47776E-05	5.8	3.20754E-05	5.8

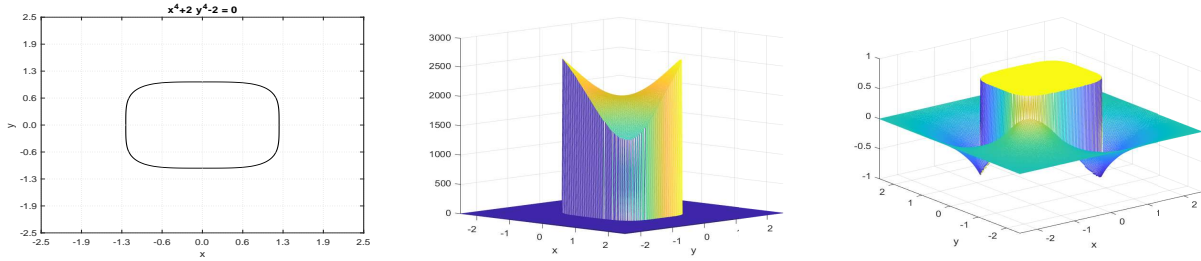


FIGURE 8. Example 3.6: the interface curve Γ_I (left), the coefficient $a(x, y)$ (middle) and the numerical solution u_h (right) with $h = 2^{-8} \times 5$, where u_h is computed by our proposed hybrid finite difference scheme. In order to show the graph of $a(x, y)$ clearly, we rotate the graph of $a(x, y)$ by $\pi/2$ in this figure.

Example 3.7. Let $\Omega = (-\pi, \pi)^2$ and the interface curve be given by $\Gamma_I := \{(x, y) \in \Omega : \psi(x, y) = 0\}$ with $\psi(x, y) = x^2 + y^2 - 2$. The functions in (1.1) are given by

$$\begin{aligned} a_+ &= 2 + \cos(x - y), & a_- &= 10^3(2 + \cos(x - y)), & g_D &= \sin(x - y) - 2, \\ f_+ &= \sin(8x) \sin(8y), & f_- &= \cos(8x) \cos(8y), & g_N &= \cos(x + y), \\ -u_x(-\pi, y) + \cos(y)u(-\pi, y) &= \cos(y) + 1, & u(\pi, y) &= 0, & \text{for } y &\in (-\pi, \pi), \\ u(x, -\pi) &= 0, & u(x, \pi) &= 0, & \text{for } x &\in (-\pi, \pi). \end{aligned}$$

Note the high contrast $a_-/a_+ = 10^3$ on Γ_I . The numerical results are presented in Table 7 and Fig. 9.

Example 3.8. Let $\Omega = (-\frac{\pi}{2}, \frac{\pi}{2})^2$ and the interface curve be given by $\Gamma_I := \{(x, y) \in \Omega : \psi(x, y) = 0\}$ with $\psi(x, y) = y^2 + \frac{2x^2}{x^2+1} - 1$. The functions in (1.1) are given by

$$\begin{aligned} a_+ &= 10^3(2 + \sin(x + y)), & a_- &= 10^{-3}(2 + \cos(x - y)), & g_D &= \sin(x) \cos(y) - 2, \\ f_+ &= \sin(6x) \sin(6y), & f_- &= \cos(6x) \cos(6y), & g_N &= \cos(x + y), \\ -u_x(-\frac{\pi}{2}, y) + \cos(y)u(-\frac{\pi}{2}, y) &= \sin(y + \frac{\pi}{2})(y - \frac{\pi}{2}), & u(\frac{\pi}{2}, y) &= 0, & \text{for } y &\in (-\frac{\pi}{2}, \frac{\pi}{2}), \end{aligned}$$

TABLE 7. Performance in Example 3.7 of our proposed hybrid finite difference scheme on uniform Cartesian meshes with $h = 2^{-J} \times 2\pi$.

J	$\ u_h - u_{h/2}\ _2$	order	$\ u_h - u_{h/2}\ _\infty$	order
4	7.02037E+02	0	1.84708E+02	0
5	9.69424E+00	6.2	2.54978E+00	6.2
6	2.26556E-01	5.4	5.97145E-02	5.4
7	2.57284E-03	6.5	6.79725E-04	6.5
8	5.07886E-05	5.7	1.34801E-05	5.7

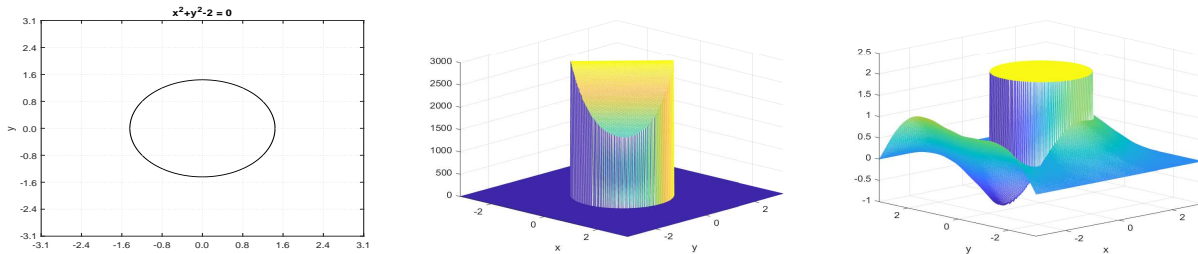


FIGURE 9. Example 3.7: the interface curve Γ_I (left), the coefficient $a(x, y)$ (middle) and the numerical solution u_h (right) with $h = 2^{-8} \times 2\pi$, where u_h is computed by our proposed hybrid finite difference scheme. In order to show the graph of $a(x, y)$ clearly, we rotate the graph of $a(x, y)$ by $\pi/2$ in this figure.

$$u(x, -\frac{\pi}{2}) = 0, \quad u(x, \frac{\pi}{2}) = 0, \quad \text{for } x \in (-\frac{\pi}{2}, \frac{\pi}{2}).$$

The high contrast $a_+/a_- \approx 10^6$ on Γ_I . The numerical results are presented in Table 8 and Fig. 10.

TABLE 8. Performance in Example 3.8 of our proposed hybrid finite difference scheme on uniform Cartesian meshes with $h = 2^{-J} \times \pi$.

J	$\ u_h - u_{h/2}\ _2$	order	$\ u_h - u_{h/2}\ _\infty$	order
5	1.17512E-01	0	1.95534E-01	0
6	1.34603E-03	6.4	5.01334E-03	5.3
7	2.97345E-05	5.5	9.62920E-05	5.7
8	3.63705E-07	6.4	1.11523E-06	6.4

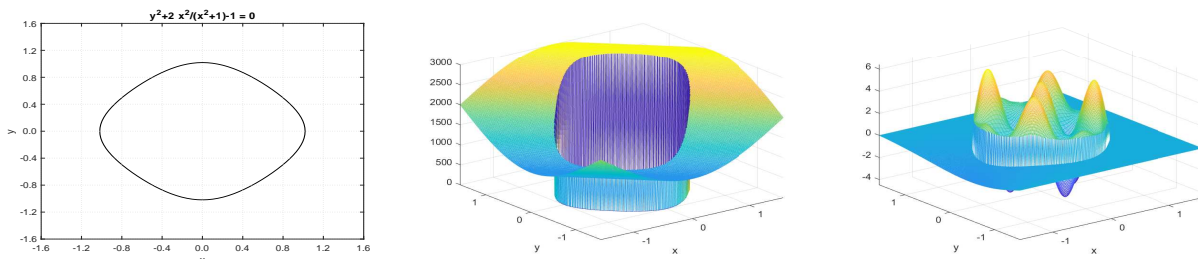


FIGURE 10. Example 3.8: the interface curve Γ_I (left), the coefficient $a(x, y)$ (middle) and the numerical solution u_h (right) with $h = 2^{-8} \times \pi$, where u_h is computed by our proposed hybrid finite difference scheme.

Example 3.9. Let $\Omega = (-2.5, 2.5)^2$ and the interface curve be given by $\Gamma_I := \{(x, y) \in \Omega : \psi(x, y) = 0\}$ with $\psi(x, y) = y^2 - 2x^2 + x^4 - \frac{1}{4}$. The functions in (1.1) are given by

$$\begin{aligned} a_+ &= 10^3(10 + \cos(x)\cos(y)), & a_- &= 10^{-3}(10 + \sin(x)\sin(y)), & g_D &= \sin(x) - 2, \\ f_+ &= \sin(4\pi x)\sin(4\pi y), & f_- &= \cos(4\pi x)\cos(4\pi y), & g_N &= \cos(y), \end{aligned}$$

$$\begin{aligned} u(-2.5, y) &= 0, & u(2.5, y) &= 0, & \text{for } y &\in (-2.5, 2.5), \\ u(x, -2.5) &= 0, & u(x, 2.5) &= 0, & \text{for } x &\in (-2.5, 2.5). \end{aligned}$$

The high contrast $a_+/a_- \approx 10^6$ on Γ_I . The numerical results are presented in Table 9 and Fig. 11.

TABLE 9. Performance in Example 3.9 of our proposed hybrid finite difference scheme on uniform Cartesian meshes with $h = 2^{-J} \times 5$.

J	$\ u_h - u_{h/2}\ _2$	order	$\ u_h - u_{h/2}\ _\infty$	order
5	6.18678E+00	0	9.88338E+00	0
6	9.69535E-02	6.0	2.17089E-01	5.5
7	1.67043E-03	5.9	3.52407E-03	5.9
8	2.43148E-05	6.1	5.22530E-05	6.1

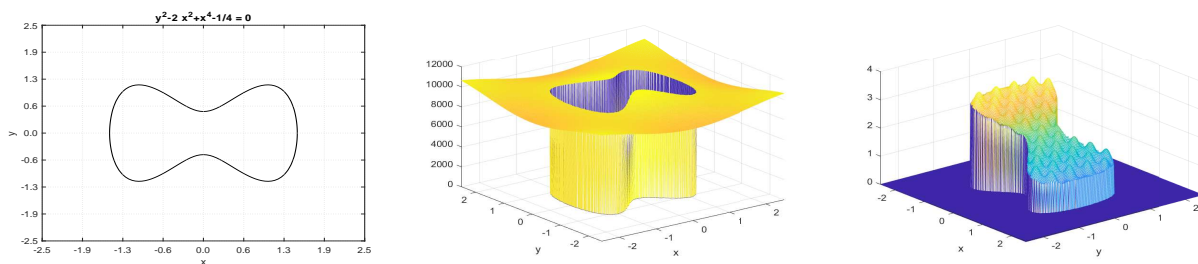


FIGURE 11. Example 3.9: the interface curve Γ_I (left), the coefficient $a(x, y)$ (middle) and the numerical solution u_h (right) with $h = 2^{-8} \times 5$. In order to show the graph of u_h clearly, we rotate the graph of u_h by $\pi/2$ in this figure.

Example 3.10. Let $\Omega = (-\pi, \pi)^2$ and the interface curve be given by $\Gamma_I := \{(x, y) \in \Omega : \psi(x, y) = 0\}$ with $\psi(x, y) = x^2 + y^2 - 4$. The functions in (1.1) are given by

$$\begin{aligned} a_+ &= 10(2 + \cos(x - y)), & a_- &= 10^{-6}(2 + \sin(x) \sin(y)), & g_D &= \sin(y) - 10, \\ f_+ &= \sin(6x) \sin(6y), & f_- &= \cos(6x) \cos(6y), & g_N &= \cos(x), \\ -u_x(-\pi, y) + \sin(y)u(-\pi, y) &= \cos(y), & u(\pi, y) &= 0, & \text{for } y &\in (-\pi, \pi), \\ -u_y(x, -\pi) &= \sin(x - \pi), & u_y(x, \pi) + \cos(x)u(x, \pi) &= \cos(x) + 1, & \text{for } x &\in (-\pi, \pi). \end{aligned}$$

The high contrast $a_+/a_- \approx 10^7$ on Γ_I . The numerical results are presented in Table 10 and Fig. 12.

TABLE 10. Performance in Example 3.10 of our proposed hybrid finite difference scheme on uniform Cartesian meshes with $h = 2^{-J} \times 2\pi$.

J	$\ u_h - u_{h/2}\ _2$	order	$\ u_h - u_{h/2}\ _\infty$	order
5	1.60217E+04	0	1.39059E+04	0
6	2.94197E+02	5.8	2.79828E+02	5.6
7	4.54676E+00	6.0	6.36193E+00	5.5
8	5.82759E-02	6.3	1.02577E-01	6.0

4. CONCLUSION

To our best knowledge, so far there were no 13-point finite difference schemes for irregular points available in the literature, that can achieve fifth or sixth order for elliptic interface problems with discontinuous coefficients. Our contributions of this paper are as follows:

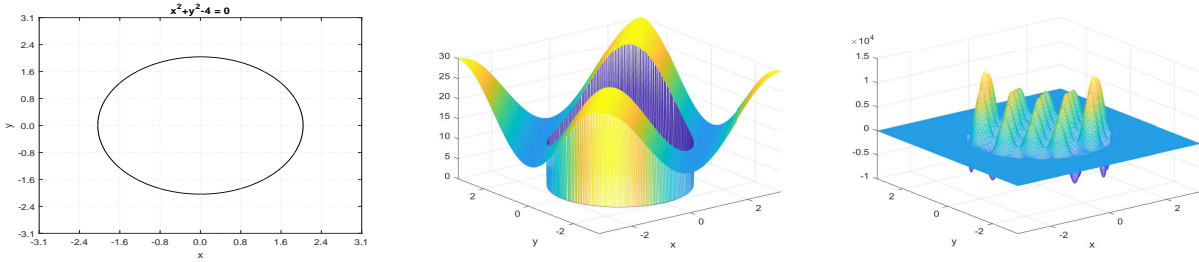


FIGURE 12. Example 3.10: the interface curve Γ_I (left), the coefficient $a(x, y)$ (middle) and the numerical solution u_h (right) with $h = 2^{-8} \times 2\pi$, where u_h is computed by our proposed hybrid finite difference scheme.

- We propose a hybrid (13-point for irregular points and compact 9-point for interior regular points) finite difference scheme, which demonstrates six order accuracy in all our numerical experiments, for elliptic interface problems with discontinuous, variable and high-contrast coefficients, discontinuous source terms and two non-homogeneous jump conditions.
- The proposed hybrid scheme demonstrates a robust high-order convergence for the challenging cases of high-contrast ratios of the coefficients a_{\pm} : $\sup(a_+)/\inf(a_-) = 10^{-3}, 10^{-6}, 10^6, 10^7$.
- Due to the flexibility and efficiency of the implementation, it is very simple to achieve the implementation for 25-point or 36-point schemes for irregular points of elliptic interface problems and Helmholtz interface equations with discontinuous wave numbers.
- From the results in Tables 1 and 2, we find that if we only replace the 13-point scheme for irregular points by a 9-point scheme, then the numerical errors increase significantly, while the condition number only slightly decreases. Thus, the proposed hybrid scheme could significantly improve the numerical performance with a slight increase in the complexity of the corresponding linear system.
- We also derive a 6-point/4-point schemes with a sixth order accuracy at the side/corner points for the case of smooth coefficients α and β in the Robin boundary conditions $\frac{\partial u}{\partial \bar{n}} + \alpha u = g_1$ and $\frac{\partial u}{\partial \bar{n}} + \beta u = g_4$.
- The presented numerical experiments confirm the sixth order of accuracy in the l_2 and l_{∞} norms of our proposed hybrid scheme.

5. APPENDIX

Let us first present the definitions of several index sets $\Lambda_{M+1}, \Lambda_{M+1}^{V,1}, \Lambda_{M+1}^{V,2}, \Lambda_{M+1}^{H,1}, \Lambda_{M+1}^{H,2}$, which are employed in Section 2. Define $\mathbb{N}_0 := \mathbb{N} \cup \{0\}$, the set of all nonnegative integers. Given $M+1 \in \mathbb{N}_0$, we use the same definitions [8, (2.4) and (2.7)] as follows:

$$\Lambda_{M+1} := \{(m, n-m) : n = 0, \dots, M+1 \text{ and } m = 0, \dots, n\}, \quad M+1 \in \mathbb{N}_0, \quad (5.1)$$

$$\Lambda_{M+1}^{V,2} := \Lambda_{M+1} \setminus \Lambda_{M+1}^{V,1} \quad \text{with} \quad \Lambda_{M+1}^{V,1} := \{(\ell, k-\ell) : k = \ell, \dots, M+1-\ell \text{ and } \ell = 0, 1\}, \quad (5.2)$$

$$\Lambda_{M+1}^{H,j} := \{(n, m) : (m, n) \in \Lambda_{M+1}^{V,j}, j = 1, 2\}. \quad (5.3)$$

For all $(m, n) \in \Lambda_{M+1}^{V,1}$, we define

$$G_{M,m,n}^V(x, y) := \sum_{\ell=0}^{\lfloor \frac{n}{2} \rfloor} \frac{(-1)^\ell x^{m+2\ell} y^{n-2\ell}}{(m+2\ell)!(n-2\ell)!} + \sum_{(m', n') \in \Lambda_{M+1}^{V,2} \setminus \Lambda_{m+n}^{V,2}} A_{m', n', m, n}^{V,u} \frac{x^{m'} y^{n'}}{m'! n'!}, \quad (5.4)$$

and for all $(m, n) \in \Lambda_{M-1}$,

$$Q_{M,m,n}^V(x, y) := \sum_{\ell=1}^{1+\lfloor \frac{n}{2} \rfloor} \frac{(-1)^\ell x^{m+2\ell} y^{n-2\ell+2}}{(m+2\ell)!(n-2\ell+2)!} \frac{1}{a^{(0,0)}} + \sum_{(m', n') \in \Lambda_{M+1}^{V,2} \setminus \Lambda_{m+n+2}^{V,2}} A_{m', n', m, n}^{V,f} \frac{x^{m'} y^{n'}}{m'! n'!}, \quad (5.5)$$

where $A_{m',n',m,n}^{V,u}$ and $A_{m',n',m,n}^{V,f}$ are constants which are uniquely determined by $\{a^{(m,n)} : (m,n) \in \Lambda_M\}$, and the floor function $\lfloor x \rfloor$ is defined to be the largest integer less than or equal to $x \in \mathbb{R}$.

For all $(m,n) \in \Lambda_{M+1}^{H,1}$, we define

$$G_{M,m,n}^H(x,y) := \sum_{\ell=0}^{\lfloor \frac{m}{2} \rfloor} \frac{(-1)^\ell y^{n+2\ell} x^{m-2\ell}}{(n+2\ell)!(m-2\ell)!} + \sum_{(m',n') \in \Lambda_{M+1}^{H,2} \setminus \Lambda_{m+n}^{H,2}} A_{m',n',m,n}^{H,u} \frac{x^{m'} y^{n'}}{m'! n'!}, \quad (5.6)$$

and for all $(m,n) \in \Lambda_{M-1}$,

$$Q_{M,m,n}^H(x,y) := \sum_{\ell=1}^{1+\lfloor \frac{m}{2} \rfloor} \frac{(-1)^\ell y^{n+2\ell} x^{m-2\ell+2}}{(n+2\ell)!(m-2\ell+2)!} \frac{1}{a^{(0,0)}} + \sum_{(m',n') \in \Lambda_{M+1}^{H,2} \setminus \Lambda_{m+n+2}^{H,2}} A_{m',n',m,n}^{H,f} \frac{x^{m'} y^{n'}}{m'! n'!}, \quad (5.7)$$

where $A_{m',n',m,n}^{H,u}$ and $A_{m',n',m,n}^{H,f}$ are constants which are uniquely determined by $\{a^{(m,n)} : (m,n) \in \Lambda_M\}$, and the floor function $\lfloor x \rfloor$ is defined to be the largest integer less than or equal to $x \in \mathbb{R}$.

In this appendix, we provide the proofs to all the technical results stated in Section 2.

Proof of Theorem 2.1. Choose $M = 6$ and replace $G_{m,n}$, $H_{m,n}$ and Λ_{M+1}^1 in [7,] by $G_{M,m,n}^V$ given in (5.4), $Q_{M,m,n}^V$ in (5.5), and $\Lambda_{M+1}^{V,1}$ in (5.2). \square

Proof of Theorem 2.2. Let $M_f = M_{g_1} = M$ in the proof of [8, Theorem 2.3]. Then [8, (4.7)] implies

$$\sum_{k=0}^1 \sum_{\ell=-1}^1 C_{k,\ell}^{\mathcal{B}_1} u(x_i + kh, y_j + \ell h) = \sum_{(m,n) \in \Lambda_{M-1}} f^{(m,n)} C_{f,m,n}^{\mathcal{B}_1} + \sum_{n=0}^M g_1^{(n)} C_{g_1,n}^{\mathcal{B}_1} + \mathcal{O}(h^{M+2}), \quad h \rightarrow 0 \quad (5.8)$$

Since $-u_x + \alpha u = g_1$ on Γ_1 , we have $u^{(1,n)} = \sum_{i=0}^n \binom{n}{i} \alpha^{(n-i)} u^{(0,i)} - g_1^{(n)}$ for all $n = 0, \dots, M$. By (2.5),

$$\begin{aligned} u(x + x_i^*, y + y_j^*) &= \sum_{n=0}^{M+1} u^{(0,n)} G_{M,0,n}^V(x,y) + \sum_{n=0}^M u^{(1,n)} G_{M,1,n}^V(x,y) + \sum_{(m,n) \in \Lambda_{M-1}} f^{(m,n)} Q_{M,m,n}^V(x,y) + \mathcal{O}(h^{M+2}) \\ &= \sum_{n=0}^{M+1} u^{(0,n)} G_{M,0,n}^V(x,y) + \sum_{n=0}^M u^{(1,n)} G_{M,1,n}^V(x,y) + \sum_{(m,n) \in \Lambda_{M-1}} f^{(m,n)} Q_{M,m,n}^V(x,y) + \mathcal{O}(h^{M+2}) \\ &= \sum_{n=0}^{M+1} u^{(0,n)} G_{M,0,n}^V(x,y) + \sum_{n=0}^M \left(\sum_{i=0}^n \binom{n}{i} \alpha^{(n-i)} u^{(0,i)} - g_1^{(n)} \right) G_{M,1,n}^V(x,y) + \sum_{(m,n) \in \Lambda_{M-1}} f^{(m,n)} Q_{M,m,n}^V(x,y) \\ &\quad + \mathcal{O}(h^{M+2}) \\ &= \sum_{n=0}^{M+1} u^{(0,n)} G_{M,0,n}^V(x,y) + \sum_{n=0}^M \sum_{i=0}^n \binom{n}{i} \alpha^{(n-i)} u^{(0,i)} G_{M,1,n}^V(x,y) - \sum_{n=0}^M g_1^{(n)} G_{M,1,n}^V(x,y) \\ &\quad + \sum_{(m,n) \in \Lambda_{M-1}} f^{(m,n)} Q_{M,m,n}^V(x,y) + \mathcal{O}(h^{M+2}) \\ &= \sum_{n=0}^{M+1} u^{(0,n)} G_{M,0,n}^V(x,y) + \sum_{i=0}^M \sum_{n=i}^M \binom{n}{i} \alpha^{(n-i)} u^{(0,i)} G_{M,1,n}^V(x,y) - \sum_{n=0}^M g_1^{(n)} G_{M,1,n}^V(x,y) \\ &\quad + \sum_{(m,n) \in \Lambda_{M-1}} f^{(m,n)} Q_{M,m,n}^V(x,y) + \mathcal{O}(h^{M+2}) \\ &= u^{(0,M+1)} G_{M,0,M+1}^V(x,y) + \sum_{n=0}^M u^{(0,n)} G_{M,0,n}^V(x,y) + \sum_{n=0}^M \sum_{i=n}^M \binom{i}{n} \alpha^{(i-n)} u^{(0,n)} G_{M,1,i}^V(x,y) - \sum_{n=0}^M g_1^{(n)} G_{M,1,n}^V(x,y) \\ &\quad + \sum_{(m,n) \in \Lambda_{M-1}} f^{(m,n)} Q_{M,m,n}^V(x,y) + \mathcal{O}(h^{M+2}), \quad \text{for } x, y \in (-2h, 2h). \end{aligned}$$

So (5.8) leads to

$$\sum_{n=0}^{M+1} u^{(0,n)} I_n^{\mathcal{B}_1} + \sum_{(m,n) \in \Lambda_{M-1}} f^{(m,n)} (J_{m,n}^{\mathcal{B}_1} - C_{f,m,n}^{\mathcal{B}_1}) + \sum_{n=0}^M g_1^{(n)} (K_n^{\mathcal{B}_1} - C_{g_1,n}^{\mathcal{B}_1}) = \mathcal{O}(h^{M+2}), \quad (5.9)$$

as $h \rightarrow 0$, where

$$\begin{aligned} I_n^{\mathcal{B}_1} &:= \sum_{k=0}^1 \sum_{\ell=-1}^1 C_{k,\ell}^{\mathcal{B}_1} \left(G_{M,0,n}^V(kh, \ell h) + \sum_{i=n}^M \binom{i}{n} \alpha^{(i-n)} G_{M,1,i}^V(kh, \ell h) (1 - \delta_{n,M+1}) \right), \\ J_{m,n}^{\mathcal{B}_1} &:= \sum_{k=0}^1 \sum_{\ell=-1}^1 C_{k,\ell}^{\mathcal{B}_1} Q_{M,m,n}^V(kh, \ell h), \quad K_n^{\mathcal{B}_1} := - \sum_{k=0}^1 \sum_{\ell=-1}^1 C_{k,\ell}^{\mathcal{B}_1} G_{M,1,n}^V(kh, \ell h), \end{aligned} \quad (5.10)$$

$\delta_{a,a} = 1$, and $\delta_{a,b} = 0$ for $a \neq b$. □

Proof of Theorem 2.3. The proof is almost identical to the proof of Theorem 2.2. □

Proof of Theorem 2.4. The proof is almost identical to the proof of Theorem 2.2. □

Proof of Theorem 2.5. The proof is similar to the proof of [8, Theorem 2.4]. Precisely, replace $\mathcal{B}_1 u = \frac{\partial u}{\partial \bar{n}} - iku = g_1$ by $\mathcal{B}_1 u = \frac{\partial u}{\partial \bar{n}} + \alpha u = g_1$ in the proof of [8, Theorem 2.4] with $M = M_f = M_{g_1} = M_{g_3} = 5$, and replace [8, $G_{M,m,n}^V$, $Q_{M,m,n}^V$, $G_{M,m,n}^H$ and $Q_{M,m,n}^H$] by (5.4), (5.5), (5.6) and (5.7). □

Proof of Theorem 2.6. The proof is similar to the proof of [8, Theorem 2.5]. Precisely, replace $\mathcal{B}_1 u = \frac{\partial u}{\partial \bar{n}} - iku = g_1$ and $\mathcal{B}_4 u = \frac{\partial u}{\partial \bar{n}} - iku = g_4$ by $\mathcal{B}_1 u = \frac{\partial u}{\partial \bar{n}} + \alpha u = g_1$ and $\mathcal{B}_4 u = \frac{\partial u}{\partial \bar{n}} + \beta u = g_4$ respectively in the proof of [8, Theorem 2.5] with $M = M_f = M_{g_1} = M_{g_4} = 5$ and replace [8, $G_{M,m,n}^V$, $Q_{M,m,n}^V$, $G_{M,m,n}^H$ and $Q_{M,m,n}^H$] by (5.4), (5.5), (5.6) and (5.7). □

Proof of Theorem 2.7. (2.28) can be obtained by $u_-^{(0,0)} = u_+^{(0,0)} - g_D^{(0,0)}$ and [7, (7.18)]. The rest of the proof is straightforward and follows from [7, (7.8), (7.10), (7.16), and (7.18)]. □

Proof of Theorem 2.8. Choose $M = 4$, replace Λ_{M+1}^1 , $G_{m,n}^\pm$, $H_{m,n}^\pm$, $d_{i,j}^\pm$ in [7, Theorem 3.3] by $\Lambda_{M+1}^{V,1}$, $G_{M,m,n}^{\pm,V}$, $Q_{M,m,n}^{\pm,V}$, $d_{i,j}^\pm \cup e_{i,j}^\pm$ in this paper. □

Proof of (2.42). Note that when we use the formulas of [7] in this proof, we need to replace Λ_{M+1}^1 , $G_{m,n}^\pm$, $H_{m,n}^\pm$, $d_{i,j}^\pm$ in [7] by $\Lambda_{M+1}^{V,1}$, $G_{M,m,n}^{\pm,V}$, $Q_{M,m,n}^{\pm,V}$, $d_{i,j}^\pm \cup e_{i,j}^\pm$ in this paper. Consider $I_{0,0}(h) = \mathcal{O}(h^{M+2})$ in [7, (3.29)]. According to [7, (3.28)] and (2.30) in this paper, $I_{0,0}(h) = \mathcal{O}(h^{M+2})$ implies

$$\sum_{(k,\ell) \in d_{i,j}^+ \cup e_{i,j}^+} C_{k,\ell}(h) G_{M,0,0}^{+,V}(v_0 h + kh, w_0 h + \ell h) + \sum_{\substack{(m',n') \in \Lambda_{M+1}^{V,1} \\ m'+n' \geq 0}} I_{m',n'}^-(h) T_{m',n',0,0}^{u+} = \mathcal{O}(h^{M+2}). \quad (5.11)$$

By (2.28), (5.11) is equivalent to

$$\sum_{(k,\ell) \in d_{i,j}^+ \cup e_{i,j}^+} C_{k,\ell}(h) G_{M,0,0}^{+,V}(v_0 h + kh, w_0 h + \ell h) + I_{0,0}^-(h) = \mathcal{O}(h^{M+2}),$$

i.e.,

$$\sum_{(k,\ell) \in d_{i,j}^+ \cup e_{i,j}^+} C_{k,\ell}(h) G_{M,0,0}^{+,V}(v_0 h + kh, w_0 h + \ell h) + \sum_{(k,\ell) \in d_{i,j}^- \cup e_{i,j}^-} C_{k,\ell}(h) G_{M,0,0}^{-,V}(v_0 h + kh, w_0 h + \ell h) = \mathcal{O}(h^{M+2}). \quad (5.12)$$

According to the proof of [7, Lemma 2.1] and (5.4),

$$G_{M,0,0}^{\pm,V}(x, y) := 1. \quad (5.13)$$

Consider the coefficients of h^i for $i = 0, 1, \dots, M + 1$ in (5.12), then (5.13) implies

$$\sum_{(k,\ell) \in d_{i,j}^+ \cup e_{i,j}^+} c_{k,\ell,i} + \sum_{(k,\ell) \in d_{i,j}^- \cup e_{i,j}^-} c_{k,\ell,i} = 0, \quad \text{for } i = 0, 1, \dots, M + 1. \quad (5.14)$$

This proves (2.42). □

REFERENCES

- [1] X. Chen, X. Feng, and Z. Li, A direct method for accurate solution and gradient computations for elliptic interface problems. *Numer. Algorithms*. **80** (2019), 709-740.
- [2] B. Dong, X. Feng, and Z. Li, An FE-FD method for anisotropic elliptic interface problems. *SIAM J. Sci. Comput.* **42** (2020), B1041-B1066.
- [3] R. Ewing, Z. Li, T. Lin, and Y. Lin, The immersed finite volume element methods for the elliptic interface problems. *Math. Comput. Simul.* **50** (1999), 63-76.
- [4] H. Feng and S. Zhao, A fourth order finite difference method for solving elliptic interface problems with the FFT acceleration. *J. Comput. Phys.* **419** (2020), 109677.
- [5] H. Feng and S. Zhao, FFT-based high order central difference schemes for three-dimensional Poisson's equation with various types of boundary conditions. *J. Comput. Phys.* **410** (2020), 109391.
- [6] Q. Feng, B. Han, and P. Minev, Sixth order compact finite difference schemes for Poisson interface problems with singular sources. *Comp. Math. Appl.* **99** (2021), 2-25.
- [7] Q. Feng, B. Han, and P. Minev, A high order compact finite difference scheme for elliptic interface problems with discontinuous and high-contrast coefficients, arXiv:2105.04600 (2021), 30 pp.
- [8] Q. Feng, B. Han, and M. Michelle, Sixth order compact finite difference method for 2D Helmholtz equations with singular sources and reduced pollution effect, arXiv:2112.07154 (2021), 20 pp.
- [9] Y. Gong, B. Li, and Z. Li, Immersed-interface finite-element methods for elliptic interface problems with nonhomogeneous jump conditions. *SIAM J. Numer. Anal.* **46** (2008), 472-495.
- [10] X. He, T. Lin, and Y. Lin, Immersed finite element methods for elliptic interface problems with non-homogeneous jump conditions. *Int. J. Numer. Anal. Model.* **8** (2011), 284-301.
- [11] K. Ito, Z. Li, and Y. Kyei, Higher-order, Cartesian grid based finite difference schemes for elliptic equations on irregular domains. *SIAM J. Sci. Comput.* **27** (2005), 346-367.
- [12] Z. Li and K. Ito, The immersed interface method: numerical solutions of PDEs involving interfaces and irregular domains. *Society for Industrial and Applied Mathematics*. 2006.
- [13] Z. Li, A fast iterative algorithm for elliptic interface problems. *SIAM J. Numer. Anal.* **35** (1998), 230-254.
- [14] Z. Li and K. Pan, Can 4th-order compact schemes exist for flux type BCs? arXiv:2109.05638 (2021), 22 pp.
- [15] R. J. Leveque and Z. Li, The Immersed interface method for elliptic equations with discontinuous coefficients and singular sources. *SIAM J. Numer. Anal.* **31** (1994), 1019-1044.
- [16] M. Nabavi, M. H. K. Siddiqui, and J. Dargahi, A new 9-point sixth-order accurate compact finite-difference method for the Helmholtz equation. *J. Sound Vib.* **307** (2007), 972-982.
- [17] K. Pan, D. He, and Z. Li, A high order compact FD framework for elliptic BVPs involving singular sources, interfaces, and irregular domains, *J. Sci. Comput.* **88** (2021), 1-25.
- [18] Y. Ren, H. Feng, and S. Zhao, A FFT accelerated high order finite difference method for elliptic boundary value problems over irregular domains. *J. Comput. Phys.* **448** (2022), 110762.
- [19] E. Turkel, D. Gordon, R. Gordon, and S. Tsynkov, Compact 2D and 3D sixth order schemes for the Helmholtz equation with variable wave number. *J. Comp. Phys.* **232** (2013), 272-287.
- [20] A. Wiegmann and K. P. Bube, The explicit-jump immersed interface method: finite difference methods for PDEs with piecewise smooth solutions. *SIAM J. Numer. Anal.* **37** (2000), 827-862.
- [21] S. Yu, Y. Zhou, and G. W. Wei, Matched interface and boundary (MIB) method for elliptic problems with sharp-edged interfaces. *J. Comput. Phys.* **224** (2007), 729-756.
- [22] S. Yu and G. W. Wei, Three-dimensional matched interface and boundary (MIB) method for treating geometric singularities. *J. Comput. Phys.* **227** (2007), 602-632.
- [23] Y. C. Zhou, S. Zhao, M. Feig, and G. W. Wei, High order matched interface and boundary method for elliptic equations with discontinuous coefficients and singular sources. *J. Comput. Phys.* **213** (2006), 1-30.
- [24] Y. C. Zhou and G. W. Wei, On the fictitious-domain and interpolation formulations of the matched interface and boundary (MIB) method. *J. Comput. Phys.* **219** (2006), 228-246.
- [25] X. Zhong, A new high-order immersed interface method for solving elliptic equations with imbedded interface of discontinuity. *J. Comput. Phys.* **225** (2007), 1066-1099.